
Training-Free Bias Mitigation by LLM-Assisted Bias Detection and Latent Variable Guidance

Jinya Sakurai*, Yuki Koyama, Issei Sato

The University of Tokyo

sakurai-jinya725@g.ecc.u-tokyo.ac.jp, koyama@pe.t.u-tokyo.ac.jp,
sato@g.ecc.u-tokyo.ac.jp

Abstract

Text-to-image (T2I) models have advanced creative content generation, yet their reliance on large uncurated datasets often reproduces societal biases. We present FairT2I, a training-free and interactive framework grounded in a mathematically principled latent variable guidance formulation. This formulation decomposes the generative score function into attribute-conditioned components and reweights them according to a defined distribution, providing a unified and flexible mechanism for bias-aware generation that also subsumes many existing ad hoc debiasing approaches as special cases. Building upon this foundation, FairT2I incorporates (1) latent variable guidance as the core mechanism, (2) LLM-based bias detection to automatically infer bias-prone categories and attributes from text prompts as part of the latent structure, and (3) attribute resampling, which allows users to adjust or redefine the attribute distribution based on uniform, real-world, or user-specified statistics. The accompanying user interface supports this pipeline by enabling users to inspect detected biases, modify attributes or weights, and generate debiased images in real time. Experimental results show that LLMs outperform average human annotators in the number and granularity of detected bias categories and attributes. Moreover, FairT2I achieves superior performance to baseline models in both societal bias mitigation and image diversity, while preserving image quality and prompt fidelity.

1 Introduction

Text-to-image (T2I) models, such as Stable Diffusion [Esser et al., 2024, Podell et al., 2023], Imagen [Imagen-Team-Google et al., 2024], and Flux [Black Forest Labs, 2024], have transformed visual content creation by allowing users to generate high-quality images from natural language descriptions. Yet, despite their accessibility and creative potential, these models inherit and amplify the biases present in large-scale web datasets [Bavalatti et al., 2025, Naik and Nushi, 2023]. When prompted with neutral descriptions, models often produce stereotypical representations such as depicting a nurse as female or a chief executive officer as male, thereby reinforcing societal inequalities [Wan et al., 2024, Mandal et al., 2024, Sandoval-Martin and Martínez-Sanzo, 2024, Zhang et al., 2024b, de Almeida and Rafael, 2024]. The increasing reuse of synthetic images in training pipelines further intensifies these biases over time [Wyllie et al., 2024, Alemohammad et al., 2023].

Many algorithmic approaches have been proposed to mitigate this problem; however, they continue to face significant practical limitations from the user’s perspective. Large-scale dataset curation is challenging to sustain over time [Bianchi et al., 2023], and most existing strategies [Kim et al., 2024, Zhang et al., 2023, Hirota et al., 2024] rely on computationally expensive fine-tuning or retraining

*Corresponding author: sakurai-jinya725@g.ecc.u-tokyo.ac.jp

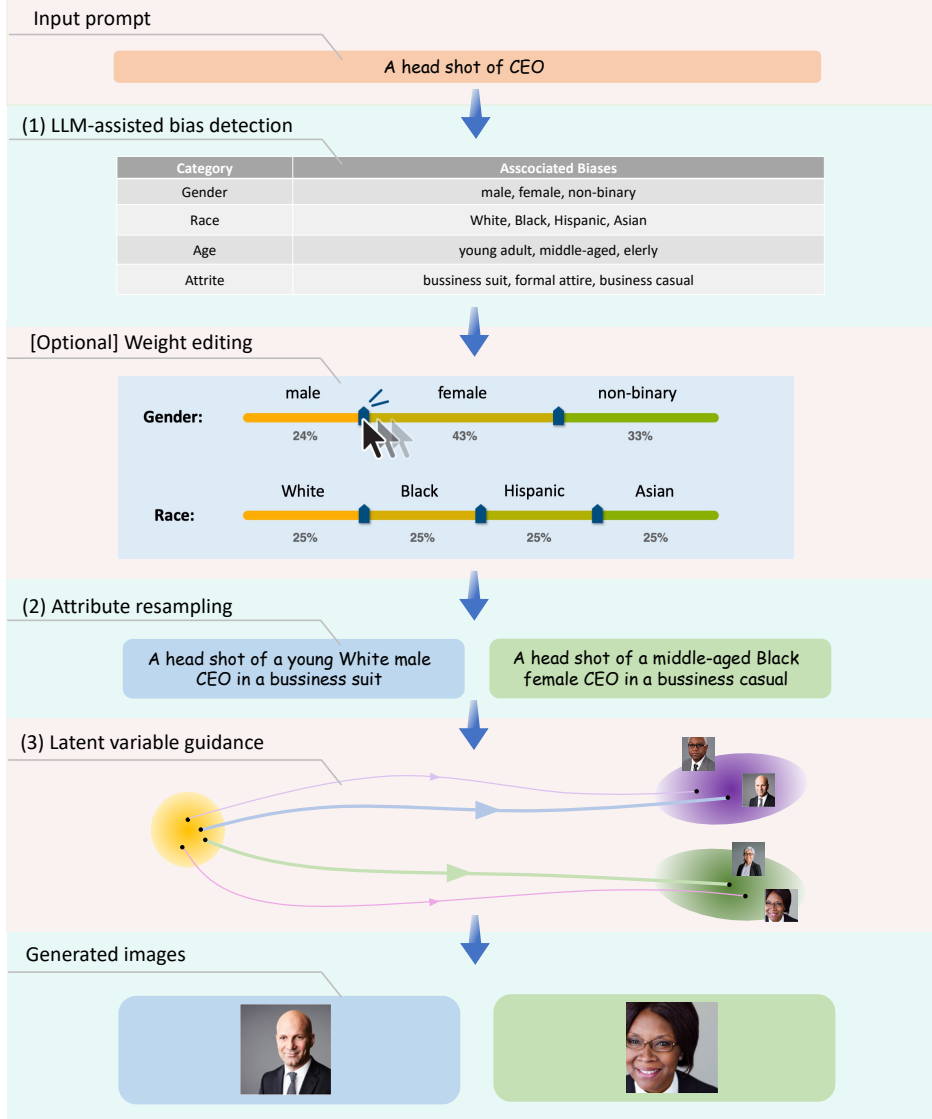


Figure 1: Overview of FairT2I. The LLM detects biases that exist in the input prompt and converts it into a set of bias-aware prompts by sampling the detected attributes from fair distributions. The interactive interface allows users to inspect, edit, and regenerate images, enabling both societal bias mitigation and improved diversity.

for each target bias, often involving delicate hyperparameter tuning [Friedrich et al., 2023]. In addition, these approaches typically depend on manually pre-defined attribute lists [Kim et al., 2024, Zhang et al., 2023, Friedrich et al., 2023], which not only constrains their adaptability to emerging or context-dependent biases but also limits the degree of user control and interpretability during deployment.

To overcome these constraints, we present *FairT2I*, a novel, theoretically grounded framework that enables bias-mitigated diffusion-based T2I process. Figure 1 illustrates the overview. FairT2I combines the reasoning ability of large language models (LLMs) with a flexible bias-aware image generation process. FairT2I operates entirely at inference time without any model fine-tuning or pre-defined attributes, allowing users to directly intervene in the debiasing process. The framework consists of three main components:

1. **LLM-based bias detection:** Given a user prompt, the LLM analyzes the text to identify implicit categories and attributes that are likely to introduce bias in generated images, such as gender,

ethnicity, or age. This transforms unstructured text into explicit bias dimensions that can be interpreted and controlled.

2. Attribute resampling: Once potential biases are identified, users can control the relative importance of each attribute (i.e., *attribute distribution*). The system supports multiple types of distributions, including a uniform distribution, one based on real-world statistics, and a custom user-specified distribution, enabling flexible control over fairness and diversity. Based on the selected distribution, the system resamples attributes to reflect the desired balance. This resampled distribution is then used to generate bias-aware prompts that explicitly encode the desired attribute composition.
3. Latent variable guidance: The image generation process is mathematically decomposed into attribute-conditioned components, and FairT2I reweights these components according to the adjusted attribute distribution. By leveraging the bias-aware prompts derived from attribute resampling, the framework realizes *latent variable guidance* in a way that is not ad hoc but theoretically grounded. This approach enables bias mitigation while maintaining fidelity and diversity in T2I, all without retraining the underlying diffusion model.

Interactive Interface for Human–AI Collaboration To support transparency and user control, we designed a web-based interface that operationalizes the bias mitigation pipeline of FairT2I. Once users give an input prompt, the system automatically detects bias categories and displays them with associated attributes. Users can then add, remove, or modify attributes and adjust their weights through sliders if desired. After confirmation, FairT2I performs attribute resampling using the bias-adjusted attribute distribution and generates a set of images. This process allows users to recognize how textual biases influence visual outcomes and provides direct agency to guide the model toward fairness or greater diversity.

Contributions The main contributions of this work are as follows.

- We introduce FairT2I, a training-free framework that integrates LLM-based bias detection with a mathematically grounded latent variable guidance formulation that factorizes the generative process into attribute-conditioned components. This is more than a simple combination of an LLM and a T2I model—our principled formulation provides a mathematical interpretation of potential sources of societal bias within the T2I generation process, offering a unified perspective that can encompass a wide range of existing ad hoc debiasing techniques.
- We design an interactive interface that allows users to visualize, modify, and control bias attributes in real time, bridging fairness research and human–AI collaboration.
- Through automatic and human-in-the-loop evaluations, we demonstrate that FairT2I outperforms baseline models in both societal bias mitigation and image diversity, while maintaining image quality and prompt fidelity.

2 Related Work

Text-to-image (T2I) models The generative capabilities of T2I models [Imagen-Team-Google et al., 2024, Esser et al., 2024, Chen et al., 2025a, Black Forest Labs, 2024] have improved dramatically through several key developments: training on large scale text image pairs [Schuhmann et al., 2022, Chen et al., 2023], architectural improvements [Peebles and Xie, 2023] from UNet [Ronneberger et al., 2015] to transformer-based designs [Vaswani et al., 2017, Dosovitskiy et al., 2020], and theoretical developments from diffusion models [Sohl-Dickstein et al., 2015, Ho et al., 2020, Song et al., 2020] to flow matching [Lipman et al., 2022, Liu et al., 2022, Lipman et al., 2024]. Furthermore, recent fine tuning approaches have significantly reduced generation time by minimizing the required number of inference steps [Liu et al., 2023, Chen et al., 2024a, Sauer et al., 2024, 2023, Yang et al., 2023]. A distinctive characteristic of state-of-the-art models is their use of separately trained components, such as Variational Auto Encoders [Kingma et al., 2014] for image compression, text encoders [Raffel et al., 2020, Radford et al., 2021], and flow model backbones, each trained on different datasets.

Societal bias in T2I models Numerous studies have investigated biases in T2I models. Research such as Ghosh and Caliskan [2023], Wu et al. [2023], Bianchi et al. [2023] highlights the biases

embedded in generated outputs for seemingly neutral input prompts that lack explicit identity- or demographic-related terms. Other works, including Cho et al. [2022], Luccioni et al. [2023] pre-define sensitive human attributes and analyze biases in outputs generated from occupational input prompts. Naik and Nushi [2023] provides broader analyses, including comparative studies with statistical data or image search results, as well as spatial analyses of generated images. Wang et al. [2023] applies methods from social psychology to explore implicit and complex biases related to race and gender. Furthermore, Luccioni et al. [2023] introduces an interactive bias analysis tool leveraging clustering methods. Lastly, Chen et al. [2024b] examines the potential for AI-generated images to perpetuate harmful feedback loops, amplifying biases in AI systems when used as training data for future models. D’Incà et al. [2024], Chinchure et al. [2023] employ LLMs to detect open-ended biases in text-to-image models where users do not have to provide predefined bias attributes.

Bias mitigation in T2I models One line of work focuses on making T2I models fair by fine-tuning or retraining various components, from the diffusion backbone [Kim et al., 2024] and text encoder Hirota et al. [2024] to postfix prompt embeddings Zhang et al. [2023] or additive residual image vectors Seth et al. [2023]. While effective, such retraining is both time- and resource-intensive and must be repeated whenever societal notions of bias evolve. By contrast, several methods eliminate societal bias only by steering generation at inference time. FairDiffusion Friedrich et al. [2023] guides sampling with randomly chosen bias attributes; [Chuang et al., 2023] removes unwanted directions from the text embedding space via calibrated projection matrices; and ENTIGEN Bansal et al. [2022] simply appends an ethical fairness postfix to the input prompt. Although these approaches require no additional training, they do depend on a predefined list of bias categories and attribute values for control.

Interactive interface for T2I generation Recent research has increasingly explored user interfaces that support interactive control and understanding of T2I generation. PromptCharm [Wang et al., 2024] introduced a mixed initiative interface that refines prompts through multi-modal feedback and visual explanations, allowing users to iteratively steer image generation with system suggestions. Promptify [Brade et al., 2023] similarly employed LLMs to recommend prompt modifications based on user feedback, enabling interactive exploration and refinement of text prompts. Beyond linguistic prompting, PromptPaint [Chung and Adar, 2023] introduced an interactive canvas that enables users to spatially compose scenes by assigning distinct text prompts to different regions of the image. PromptMap [Adamkiewicz et al., 2025] shifted the focus from control to sensemaking, visualizing the branching structure of prompt evolution as a map to help users navigate and reflect on their creative process. Expadora [Choi et al., 2025] extended these ideas to structured exploration, allowing users to specify design intentions and desired diversity levels to automatically generate a wide range of prompt variations. Collectively, these systems emphasize human agency, transparency, and creativity in T2I interaction. In contrast, FairT2I focuses on societal bias detection and mitigation, offering an interface that reveals and allows direct manipulation of latent bias attributes, thereby bridging algorithmic fairness and interactive generative control.

3 Methodologies

In this section, we present FairT2I, a mathematically grounded framework for mitigating societal biases in text-to-image (T2I) generation. At its core, our approach introduces a latent variable guidance formulation that factorizes the generative process into attribute-conditioned components, making explicit how sensitive attributes influence image generation and enabling principled bias control within the model. Building upon this foundation, we incorporate (1) an LLM-based bias detection mechanism that infers bias-prone categories and attributes directly from input prompts without relying on predefined attribute sets, and (2) an attribute resampling module that redefines attribute distributions, for example according to real-world demographic statistics, to rebalance outputs and steer generation toward greater fairness.

3.1 Preliminaries: Classifier-Free Guidance

In diffusion models [Ho et al., 2020, Sohl-Dickstein et al., 2015] and flow matching models [Esser et al., 2024, Lipman et al., 2022], classifier-free guidance [Ho and Salimans, 2022] is a powerful tool for sampling images x conditioned on a text input y . It accomplishes this by guiding an uncon-

ditional image generation model using the score function $\nabla_{\mathbf{x}} \log p(\mathbf{x})$. This enables the sampling from

$$p_w(\mathbf{x}, \mathbf{y}) \propto p(\mathbf{x})p(\mathbf{y} \mid \mathbf{x})^w \propto p(\mathbf{x})^{1-w}p(\mathbf{x} \mid \mathbf{y})^w$$

where $w \in \mathbb{R}$ is the guidance scale typically used with $w > 1$. The score satisfies

$$\nabla_{\mathbf{x}} \log p_w(\mathbf{x}, \mathbf{y}) = (1 - w)\nabla_{\mathbf{x}} \log p(\mathbf{x}) + w\nabla_{\mathbf{x}} \log p(\mathbf{x} \mid \mathbf{y})$$

so by training the network to predict both the unconditional score $\nabla_{\mathbf{x}} \log p(\mathbf{x})$ and conditional score $\nabla_{\mathbf{x}} \log p(\mathbf{x} \mid \mathbf{y})$, flexible sampling from the conditional distribution can be achieved through a weighted sum of the network outputs.

Whereas in classifier-free guidance, the weights for the score functions are typically set to achieve a trade-off between sample quality and text fidelity, our formulation 3 sets these weights to ensure fair image generation.

3.2 Latent Variable Guidance for Bias Mitigation

In latent variable guidance, societal bias is controlled by decomposing the network’s predicted score function into a weighted sum of component score functions, each conditioned on a distinct latent variable. These weights are then adjusted to enforce fairness in the generated outputs. Central to our formulation is the following proposition.

Proposition 1. *Let \mathbf{y} represent the input text, \mathbf{x} the generated image, and \mathbf{z} a discrete latent variable taking values in a finite set \mathcal{Z} , and assume conditional independence between \mathbf{x} and \mathbf{z} given \mathbf{y} , the following equation holds:*

$$\nabla_{\mathbf{x}} \log p(\mathbf{x} \mid \mathbf{y}) = \sum_{z \in \mathcal{Z}} p(\mathbf{z} = z \mid \mathbf{y}) \nabla_{\mathbf{x}} \log p(\mathbf{x} \mid \mathbf{z} = z, \mathbf{y}). \quad (1)$$

Proof. See Appendix A. □

This formulation, presented in Equation (1), effectively decomposes the score function guiding the image generation process. It explicitly separates the influence of the latent attribute \mathbf{z} (which is sampled according to its conditional probability $p(\mathbf{z} \mid \mathbf{y})$) from the subsequent image generation step, which is guided by both this sampled attribute \mathbf{z} and the original input text \mathbf{y} . This perspective allows us to contextualize existing bias mitigation strategies. Approaches such as replacing text encoders with fair alternatives [Hirota et al., 2024, Chuang et al., 2023], learning fair prompt embeddings [Zhang et al., 2023], or randomly sampling sensitive attributes [Friedrich et al., 2023] can all be interpreted as methods that implicitly or explicitly substitute the T2I model’s original, potentially biased distribution $p_{\text{bias}}(\mathbf{z} \mid \mathbf{y})$ with a more equitable target distribution $p_{\text{fair}}(\mathbf{z} \mid \mathbf{y})$. Figure 2 illustrates the generation process with latent variable guidance, compared to the standard process without it, for an input prompt $\mathbf{y} = \text{A CEO}$ and an attribute set $\mathcal{Z} = \{z_1 = \text{male}, z_2 = \text{female}\}$. In the standard setting, images are denoised at each timestep under the biased distribution $p_{\text{bias}}(\mathbf{z} \mid \mathbf{y})$, which tends to steer the generation toward male CEO representations. In contrast, latent variable guidance enables the replacement of $p_{\text{bias}}(\mathbf{z} \mid \mathbf{y})$ with a fair distribution $p_{\text{fair}}(\mathbf{z} \mid \mathbf{y})$, allowing the generation process to be steered toward more balanced and fair outcomes.

In practice, computing the summation over all possible values of z in Equation (1) can be computationally prohibitive, especially when dealing with a large or continuous space of latent attributes. To overcome this computational challenge, we employ Monte Carlo sampling from the distribution $p(\mathbf{z} \mid \mathbf{y})$. Specifically, we approximate the expectation in Equation (1) using a finite number of samples. For the simplest case, using an approach with a single sample, this approximation becomes:

$$\nabla_{\mathbf{x}} \log p(\mathbf{x} \mid \mathbf{y}) \approx \nabla_{\mathbf{x}} \log p(\mathbf{x} \mid \tilde{\mathbf{z}}, \mathbf{y}), \text{ where } \tilde{\mathbf{z}} \sim p(\mathbf{z} \mid \mathbf{y}).$$

While this approach using a single sample provides an unbiased estimate of the true score, it may exhibit higher variance compared to the exact summation. This variance can be mitigated by using additional samples; however, this benefit comes at the cost of increased computation time. Consequently, a careful trade-off between computational efficiency and the accuracy of the score estimation must be considered when implementing this approach in practical scenarios.

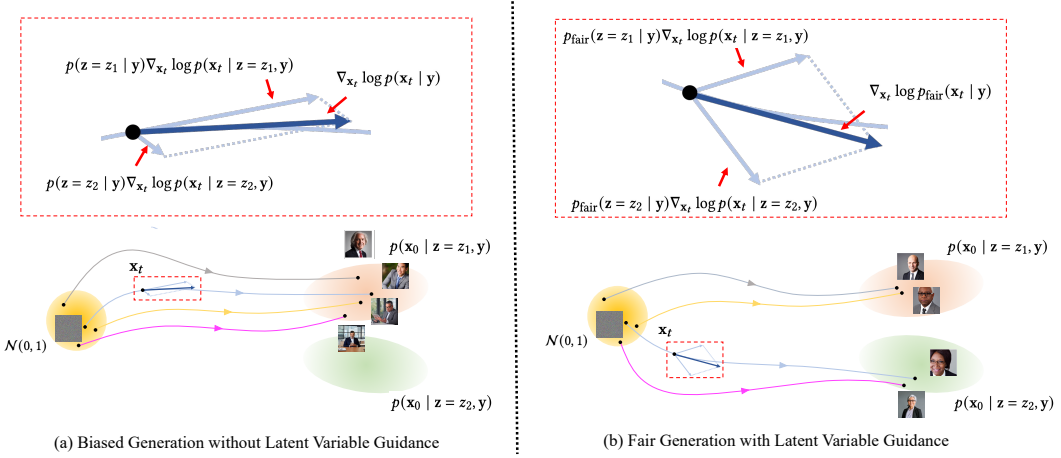


Figure 2: Comparison of generation processes without (left) and with (right) latent variable guidance for the input prompt $y = A \text{ CEO}$ and attribute set $\mathcal{Z} = \{z_1 = \text{male}, z_2 = \text{female}\}$. In the standard diffusion process, the model internalizes societal biases from the training data and denoises images toward male CEO representations, resulting in biased outputs. Latent variable guidance enables the adjustment of the denoising direction based on a fair attribute distribution, thereby allowing the mitigation of such biases in the generated results.

3.3 LLM-Assisted Bias Detection

To implement latent variable guidance, we need to define a candidate set of biases \mathcal{Z} . The simplest approach is to predefine a closed set of biases, such as race and gender; however, this approach has several limitations. For instance, one significant limitation relates to computational challenges. The diversity of input prompts is virtually infinite, meaning that a predefined set of latent attributes \mathcal{Z} can only appropriately handle a limited subset of these cases. Consequently, it is practically impossible to predefine a suitable \mathcal{Z} for every conceivable prompt in advance. Another limitation concerns incomplete representation. If the latent attribute set \mathcal{Z} is defined manually in a rule-based manner, it may fail to fully capture the diversity and context of the real world. This approach also risks overlooking biases embedded in the input text that are beyond human recognition.

To address these challenges, we leverage large language models (LLMs) [OpenAI et al., 2024, Anthropic, 2025] to automatically detect biases in the input text, as with existing bias detection methods [D’Incà et al., 2024, Chinchure et al., 2023]. Specifically, we use the LLM to predict the set of possible latent attributes \mathcal{Z} from the input text y . LLMs are prompted to output a set of latent attributes that are likely to appear in images generated by T2I models with the input text in a JSON format. This approach allows us to handle a broader range of input prompts and to detect biases that may not be apparent to human annotators.

3.4 Attribute Resampling

When we have a set of latent attributes \mathcal{Z} from LLM as potential biases in the input prompts, we can formulate $p_{\text{fair}}(\mathbf{z} = \mathbf{z} | \mathbf{y})$ to perform sampling that mitigates bias. We consider two approaches to defining $p_{\text{fair}}(\mathbf{z} = \mathbf{z} | \mathbf{y})$.

Uniform distribution One simple approach is to set the distribution of latent attributes to be uniform across all possible values of z : $p_{\text{fair}}(\mathbf{z} = \mathbf{z} | \mathbf{y}) = \frac{1}{|\mathcal{Z}|}$, which corresponds to simply mixing the scores $\nabla_{\mathbf{x}} \log p(\mathbf{x} | \mathbf{z} = \mathbf{z}, \mathbf{y})$ with equal proportions across all possible values of z . This formulation coincides with that of Fair Diffusion [Friedrich et al., 2023].

Employment statistics Research has shown that T2I models tend to exaggerate demographic stereotypes beyond what we observe in real-world distributions across various latent attributes [Naik and Nushi, 2023]. One way to address this issue is to incorporate real-world statistical data as

$p_{\text{fair}}(\mathbf{z} = z \mid \mathbf{y})$, ensuring that the generated image distributions are at least as balanced as real-world demographics.²

Upon sampling the latent attribute z from the fair conditional distribution $p_{\text{fair}}(\mathbf{z} = z \mid \mathbf{y})$, we need to compute the score $\nabla_{\mathbf{x}} \log p(\mathbf{x} \mid \mathbf{z} = z, \mathbf{y})$. To enforce that the T2I model incorporates the sampled attribute z , we use an LLM to naturally fuse the textual input \mathbf{y} and the latent attribute \mathbf{z} , and feed this augmented text $\mathbf{y} \oplus \mathbf{z}$ directly into the T2I model in place of \mathbf{y} .

4 Evaluation of LLM-Detected Bias Categories

This section evaluates the bias categories and attributes surfaced by the LLM, using human-annotated lists as a reference.

4.1 Experimental Settings

Evaluation dataset We used two datasets for this study: one for assessing societal biases in professions and another for examining potential biases in more diverse textual prompts. To evaluate occupational bias, we used the Stable Bias profession dataset [Luccioni et al., 2023], which contains 131 occupations collected from the U.S. Bureau of Labor Statistics (BLS) (see Appendix A of Luccioni et al. [2023] for full details). To probe broader forms of bias, we adopt the Parti Prompt dataset [Yu et al., 2022], which includes more than 1,600 English prompts designed to evaluate text-to-image generation models and test their limitations. For efficiency, we randomly sample 50 prompts from each dataset, with the selected subset listed in subsection B.1.

LLMs for Bias Detection We used Claude 3.7-sonnet for LLM-assisted bias detection, following a small pilot study that compared GPT-4o OpenAI et al. [2024], Claude 3.7-sonnet Anthropic [2025], Llama 3.3 Grattafiori et al. [2024], and DeepSeek V3 Liu et al. [2024]. Further details of this pilot study are provided in the appendix Appendix B.

4.2 Human Annotation and Reference Set Construction

To establish a human reference for bias categories, we conducted an annotation study using the same prompts as in the evaluation datasets. 100 text prompts, consisting of 50 prompts from the Stable Bias dataset [Luccioni et al., 2023] and 50 prompts from the PartiPrompts dataset [Yu et al., 2022] were divided into five groups of 20 prompts, with each group assigned to five independent annotators (25 participants in total). Annotators were instructed to list potential bias *categories* (e.g., gender, race, attire) along with multiple *attributes* per category (e.g., male, female, non-binary for gender). Clear format guidelines and illustrative examples were provided to ensure consistency. To maintain parity, the same few-shot examples were used both in the human instructions and in the system prompts provided to the LLMs.

For each prompt, we consolidated the five human responses by normalizing synonyms (e.g., *ethnicity* \rightarrow *race*) and merging duplicates. The resulting union of all annotators produced a single consolidated human reference set of categories and attributes per prompt. Full details of the instructions, interface, and annotation guidelines are provided in subsection B.3.

4.3 Results and Discussion

Categories and attributes To assess the ability to cover a broad range of bias categories and attributes, we compared the number of detected categories and attributes. Figure 3 presents results for the Stable Bias dataset (left) and the Parti Prompt dataset (right), showing the average of five annotators (human mean; blue), the consolidated union of all annotators (human union; orange), and the LLM outputs (green). On the Stable Bias dataset, the human union and the LLM produced a comparable breadth of categories (9.18 vs. 9.06 on average), although the LLM generated more attributes per category (4.54 vs. 3.84). On the Parti Prompt dataset, however, humans (union) enumerated more categories than the LLM (10.52 vs. 8.44), while the LLM provided denser attribute

²It is worth noting that real-world occupational distributions often reflect systemic biases and unequal access to opportunities, shaped by historical and societal factors such as limited access to education or workplace discrimination. These disparities highlight that real-world distributions are not inherently fair.

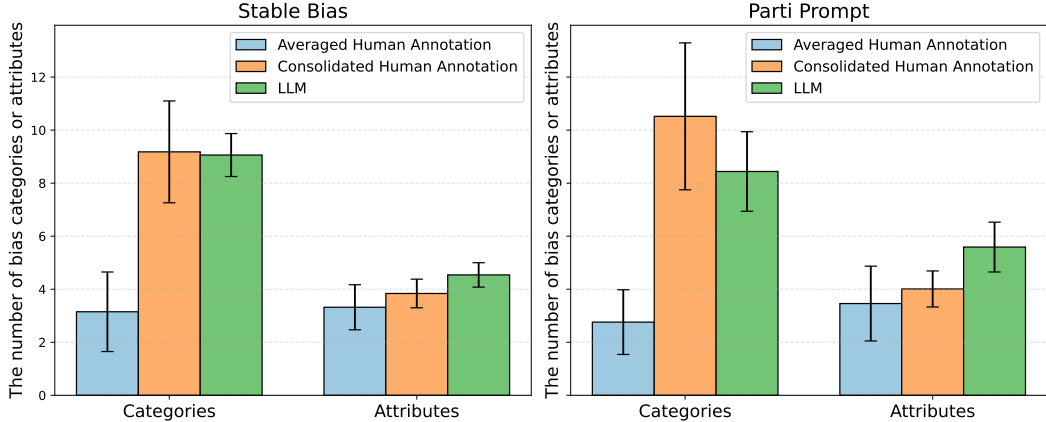


Figure 3: Number of detected categories and attributes per category for the Stable Bias (left) and Parti Prompt (right) datasets. Bars show Human Mean (blue), Human Union (orange), and LLM (green), with error bars indicating one standard deviation.

Table 1: Gender and race attribute sets on the Stable Bias dataset. Few-shot examples show the categories provided in the annotation instructions and LLM prompt. Rows report the most frequent, minimum, and maximum sets for the human union and the LLM. Numbers in parentheses indicate the number of prompts in which the set occurred. For race, humans did not annotate the category in 4 prompts.

	Gender	Race
Few-shot examples	non-binary, female, male	White, Asian, Black, Hispanic
Human Union		
Most frequent	non-binary, female, male (29/50)	White, Asian, Black, Hispanic (16/50)
Minimum	non-binary, female, male	None
Maximum	non-binary, other, male, les, gay, female	Mixed, Asian, Hispanic, African-American, Arab, African, White, Native-American, Black
LLM		
Most frequent	non-binary, female, male (46/50)	Middle Eastern, Asian, Hispanic, White, Indigenous, Black (13/50)
Minimum	non-binary, female, male	Middle Eastern, Asian, Hispanic, White, Black
Maximum	non-binary, female, androgynous, male	Middle Eastern, Asian, White, Hispanic/Latino, South Asian, Indigenous, Black

lists (5.59 vs. 4.01). Notably, the human mean values are consistently lower than both the union and the LLM (for example, only 2.76 categories and 3.46 attributes in Parti Prompt), reflecting high inter-annotator variability. Taken together, these findings suggest that, while humans provide greater breadth when aggregated, LLMs offer more consistent depth within categories.

Societal biases. Table 1 illustrates the gender and race attribute sets detected on the Stable Bias dataset. On average, human consolidation yielded 3.52 gender attributes and 5.34 race attributes per prompt, while the LLM produced 3.08 and 5.8, respectively. Both humans and the LLM frequently reproduced the few-shot examples given in the annotation instructions, but diverged in their extensions: humans showed higher variability and occasionally omitted race altogether (4 prompts), whereas the LLM produced more systematic expansions that consistently included race.

Overall, the findings indicate that LLM-based bias detection consistently outperforms average human annotators and achieves coverage comparable to the consolidated union of multiple annotators. This suggests that LLMs can serve as reliable bias detectors, offering both scalability and consistency, and their use is justified as a practical alternative to extensive human annotation.

5 Experiments: Societal Bias Mitigation

In this section, we evaluate FairT2I against existing methods using automatic metrics and human studies, demonstrating the detection of diverse textual biases and the corresponding mitigation in outputs.

5.1 Automatic Evaluation

Evaluation dataset To evaluate societal bias in professions, we use the same Stable Bias profession dataset [Lucioni et al., 2023] introduced in section 4, which contains 131 occupations from the U.S. Bureau of Labor Statistics (BLS). We consider two target distributions: (1) the uniform distribution over categories defined in FairFace [Karkkainen and Joo, 2021], and (2) BLS occupational statistics. For the uniform distribution, we used the same subset of 50 randomly sampled occupations from this dataset as in section 4. The selected subset of prompts is listed in subsection B.1. For the BLS statistics, we use the five occupation prompts mentioned in Naik and Nushi [2023]: *CEO, doctor, computer programmer, nurse, and house keeper*. As in Zhang et al. [2023], each profession is prefixed with “A headshot of ” to form an input prompt.

Evaluation metrics Following Hirota et al. [2024], Chuang et al. [2023], we measure bias in the generated outputs by computing the statistical parity [Choi et al., 2020] between the empirical distribution and the ideal target distribution. In line with Naik and Nushi [2023], we detect faces in the generated images using dlib [King, 2015] and then predict the attributes of each image using classifiers trained on the FairFace dataset [Karkkainen and Joo, 2021]. Statistical parity is defined as the ℓ_2 -distance between two probability vectors. Specifically, let $\mathbf{p} = (p_1, p_2, \dots, p_n)$, $\mathbf{q} = (q_1, q_2, \dots, q_n)$ be two distributions over n outcomes. Then the statistical parity between \mathbf{p} and \mathbf{q} is

$$SP(\mathbf{p}, \mathbf{q}) = \|\mathbf{p} - \mathbf{q}\|_2 = \sqrt{\sum_{i=1}^n (p_i - q_i)^2}.$$

A lower statistical parity indicates that the distribution of generated images more closely matches the target (fair) distribution.

For each prompt in our subset, we generate 200 images, classify each by its FairFace attribute, and compute statistical parity. Further details appear in subsection C.1.

Methods for comparison We compare FairT2I against existing debiasing methods that do not require any model finetuning:

- **Original**: the unmodified Stable Diffusion model [Rombach et al., 2022a], with no bias mitigation.
- **ENTIGEN** [Bansal et al., 2022]: appending an ethical injection phrase to the end of the prompt.
- **Fair Diffusion** [Friedrich et al., 2023]: randomly sampling attributes from a predefined bias set and applying semantic guidance [Brack et al., 2023].

Detailed hyperparameter settings for each method are provided in subsection C.2 and subsection C.3, respectively. To ensure a fair comparison, the T2I model was standardized to Stable Diffusion 1.5 [Rombach et al., 2022b] across all baseline and proposed methods.

Implementation details We used Stable Diffusion 1.5 [Rombach et al., 2022b] as our T2I model. This choice was made because the hyperparameter settings and text encoders of the comparison methods were not compatible with the newer T2I architectures [Esser et al., 2024]. We employed Claude 3.7-sonnet [Anthropic, 2025] for LLM-assisted bias detection, and GPT4o-mini [OpenAI et al., 2024] to fuse the textual input \mathbf{y} with the sensitive attribute \mathbf{z} . The parameter settings for image generation and the exact prompts supplied to the LLM are detailed in subsection C.4.

Table 2: Biased attributes associated with the input text “*a headshot of a psychologist*” as generated by LLM.

Attribute Category	Associated Biases
Gender	male, female, non-binary
Race	White, Black, Asian, Hispanic, Middle Eastern, Other
Age	young adult, middle-aged, elderly
Attire	formal business attire, casual professional, white coat, sweater with blazer
Accessories	glasses, no glasses, jewelry, no jewelry
Facial Hair	beard, mustache, clean-shaven
Hair Style	short, long, balding, styled, natural
Setting	office, bookshelf background, plain background, clinical setting
Expression	serious, smiling, attentive, compassionate

Targeting uniform distribution Table 3 reports the SP scores comparing empirical and uniform distributions of gender and race in the Stable Bias Profession subset. FairT2I most closely matches the uniform baseline on both metrics. It demonstrates that, compared to existing methods, FairT2I generates data for each attribute with greater uniformity. See Appendix C for bar-chart comparisons and more details.

Table 2 summarizes the attribute categories (race, gender, age, background, pose, and more) and the biases detected by the LLM for the prompt “*a headshot of a psychologist*”. Figure 8 then presents randomly selected outputs from each method. While the baseline methods reproduce skewed or homogeneous attribute distributions, FairT2I addresses the biases listed in Table 2, yielding high-quality headshots with balanced diversity across race, gender, accessories (e.g., glasses), and backgrounds.

Targeting BLS statistics. Table 4 summarizes the gender and race SP scores between BLS statistics for *CEO*, *computer programmer*, *doctor*, *nurse*, and *housekeeper* prompts across four methods. FairT2I consistently achieves the lowest gender SP, outperforming ENTIGEN and FairDiffusion by large margins. For race SP, FairT2I yields the best scores on *CEO*, *computer programmer*, and *housekeeper*. These results confirm that FairT2I can also steer the generated distributions toward specified target distributions. See subsection C.8 for bar-chart comparisons and further details.

Table 3: Statistical Parity of Gender and Race Distributions by the original Stable Diffusion, ENTIGEN, FairDiffusion, and FairT2I (Ours).

Method	Gender SP ↓	Race SP ↓
Original	0.2056	0.3907
ENTIGEN	0.0661	0.2001
FairDiffusion	0.2083	0.3137
FairT2I	0.0123	0.1864

6 Experiments: Diversity Control

In this section, we evaluate FairT2I not only for its ability to mitigate societal bias but also for its capacity to enhance the diversity of generated images. We conduct both quantitative (automatic) and qualitative (human) evaluations to assess the effectiveness of our method.

6.1 Experimental Settings

Evaluation dataset We employ the Parti Prompt dataset [Yu et al., 2022], which comprises over 1,600 diverse English prompts intended to rigorously evaluate T2I generation models and probe their limitations. In this work, we focus on the uniform prompt distribution, as no particular target distribution is assumed. For practical efficiency, we randomly sample 50 prompts from the full dataset as in section 4. The selected subset of prompts is listed in subsection B.1.

Models and baselines We compare FairT2I against classifier-free guidance (CFG) [Ho and Salimans, 2022] at three guidance scales (7.0, 4.0, 1.0), which modulate the trade-off between image fidelity and diversity.

Table 4: Gender Statistical Parity (top) and Race Statistical Parity (bottom) scores (lower is better) between BLS statistics for CEO, computer programmer, doctor, nurse and housekeeper in images from the original Stable Diffusion, ENTIGEN, FairDiffusion and FairT2I (Ours). For each metric and occupation, the best score is shown in bold.

Method	Gender SP ↓				
	CEO	comp. prog.	doctor	nurse	housekeeper
Original	0.3637	0.1651	0.3843	0.1796	0.1459
ENTIGEN [Bansal et al., 2022]	0.3748	0.0569	0.1229	0.1210	0.0121
FairDiffusion [Friedrich et al., 2023]	0.1956	0.1089	0.1138	0.1653	0.1597
FairT2I (Ours)	0.0710	0.0170	0.0550	0.0537	0.0121

Method	Race SP ↓				
	CEO	comp. prog.	doctor	nurse	housekeeper
Original	0.6050	0.2213	0.2110	0.1971	1.0207
ENTIGEN [Bansal et al., 2022]	0.5004	0.6115	0.4727	0.4805	0.9341
FairDiffusion [Friedrich et al., 2023]	0.1664	0.1484	0.0750	0.1285	0.3074
FairT2I (Ours)	0.0677	0.0885	0.1137	0.1541	0.2001

Table 5: Comparison of classifier-free guidance (CFG) at guidance scales 7.0, 4.0, and 1.0 and of FairT2I on the FID, CLIPScore, CLIP Trace, and BLIP2 Trace metrics. A guidance scale of 1.0 corresponds to generation without CFG.

Method	FID ↓	CLIPScore ↑	CLIP Trace ↑	BLIP2 Trace ↑
CFG-7.0	27.13	29.84	11.66	247.01
CFG-4.0	26.46	30.09	11.87	250.24
No CFG (CFG-1.0)	34.47	28.06	21.05	473.64
FairT2I (Ours)	26.24	28.35	19.18	454.49

Implementation details We use Stable Diffusion 3.5-large [Esser et al., 2024] as the T2I model. We employ Claude 3.7-sonnet [Anthropic, 2025] for LLM-assisted bias detection, and GPT-4o-mini [OpenAI et al., 2024] to fuse textual input y with sensitive attribute z . Generation hyperparameters and LLM prompts are in subsection D.2.

6.2 Automatic Evaluation

Automatic metrics and generation protocol To assess image fidelity, we compute the Fréchet Inception Distance (FID) [Heusel et al., 2017] on the COCO Karpathy test split [Lin et al., 2014]. To evaluate text–image alignment, we report CLIPScore [Hessel et al., 2021] between each generated image and its input prompt. To quantify diversity, we embed all generated images into CLIP [Radford et al., 2021] and BLIP2 [Li et al., 2023] feature spaces, compute the covariance of embeddings, and use its trace as the diversity metric. For each prompt, we generate 200 images and compute these metrics accordingly.

Results Table 5 presents quantitative evaluations in terms of FID, CLIPScore, CLIP Trace and BLIP2 Trace, illustrating the trade-off between image fidelity, text alignment and diversity. Under CFG 7.0 and CFG 4.0, FID values are low but Trace metrics remain small. By contrast, CFG 1.0 yields a high Trace value at the expense of elevated FID. Unlike these existing methods, FairT2I achieves low FID and high Trace without substantially reducing CLIPScore. Table 6 lists the attribute categories and biases detected by LLM for the prompt “*an airplane flying into a cloud that looks like a monster.*” in the Parti Prompts dataset. Figure 4 then presents the images generated by each method for the same prompt. While classifier-free guidance cannot achieve both image quality and diversity, FairT2I succeeds on both measures.

Table 6: Attribute categories and their associated options generated by LLM for the input text “*an airplane flying into a cloud that looks like monster*.”

Attribute Category	Associated Biases
Type of Airplane	commercial airliner, private jet, military aircraft, propeller plane, biplane
Cloud Appearance	dark and menacing, fluffy and cute, wispy and ethereal
Monster Type	dragon-like, humanoid, tentacled creature, multi-eyed beast, fanged monster
Time of Day	daytime, sunset, night, dawn
Weather Conditions	clear sky, stormy, partly cloudy
Viewing Angle	from below, from above, side view, frontal view
Artistic Style	photorealistic, cartoonish, dramatic, whimsical, ominous
Color Palette	bright and colorful, dark and moody, pastel, monochromatic
Sky Background	clear blue, sunset colors, stormy gray, gradient



Figure 4: Generated images for the input text “*an airplane flying into a cloud that looks like monster*.” by classifier-free guidance (CFG) at guidance scales 7.0, 4.0, and 1.0 and FairT2I (Ours). A guidance scale of 1.0 corresponds to generation without CFG.

6.3 Human Evaluation

To complement the automatic metrics, we conducted a human evaluation to assess the perceptual diversity, image quality, and text–image alignment of FairT2I in comparison with baseline methods.

Setup. For each prompt in the 50-prompt subset of the Parti Prompt dataset, we generated nine images using each of four methods: CFG-1.0, CFG-4.0, CFG-7.0, and FairT2I. All images were arranged in 3×3 grids per method, enabling side-by-side comparison across methods.

Task design To keep the annotation time manageable, the 50 prompts were divided into five tasks, each containing ten prompts and the corresponding generations from all four methods. Each task required roughly 20 minutes to complete. We recruited a total of 100 annotators, resulting in 20 independent raters per prompt.

Procedure Annotators were asked to rate every image on a five-point absolute Likert scale (1 = worst, 5 = best) along three criteria:

1. **Diversity:** How different the multiple images from the same model look for the same prompt. High diversity means the images show clearly different variations (e.g., viewpoint, layout, details), while low diversity means the images look nearly identical.
2. **Image Quality:** How clear, coherent, and visually convincing the image looks within its intended style. High-quality images are sharp, well-structured, and free from obvious AI artifacts (e.g., severe distortions, broken anatomy, unnatural textures), even if the content is fantastical or stylized (e.g., anime, surreal objects).
3. **Text Alignment:** How well the generated image matches the prompt in terms of objects, attributes, and relationships.

Detailed screenshots of the annotation interface, instructions, and answer forms are provided in Appendix D.5.

Table 7: Human evaluation summary statistics for each task and model.

Criteria	Model	Mean	Std.
Diversity	CFG-1.0	3.416	1.120
	CFG-4.0	2.697	1.154
	CFG-7.0	2.735	1.226
	FairT2I	3.643	1.105
Quality	CFG-1.0	2.775	1.152
	CFG-4.0	3.686	0.934
	CFG-7.0	3.751	1.022
	FairT2I	3.827	0.991
Alignment	CFG-1.0	3.152	1.214
	CFG-4.0	3.833	1.051
	CFG-7.0	3.862	1.096
	FairT2I	3.682	1.123

Table 8: One-sided Mann–Whitney U test results (H_1 : FairT2I > Baseline). Findings indicate whether FairT2I achieved a significantly higher score ($p < 0.001$).

Criteria	Baseline	p-value	Findings
Diversity	CFG-1.0	3.54×10^{-6}	Significant ↑
	CFG-4.0	5.90×10^{-68}	Significant ↑
	CFG-7.0	6.66×10^{-60}	Significant ↑
Quality	CFG-1.0	1.44×10^{-87}	Significant ↑
	CFG-4.0	4.74×10^{-5}	Significant ↑
	CFG-7.0	3.93×10^{-2}	Not significant
Alignment	CFG-1.0	4.97×10^{-23}	Significant ↑
	CFG-4.0	9.98×10^{-1}	Not significant
	CFG-7.0	1.00×10^0	Not significant

Results Table 7 and Table 8 summarize the outcomes of the human evaluation. Inter-annotator agreement was modest but acceptable for aggregation (Krippendorff’s α : Diversity 0.241, Quality 0.141, Alignment 0.136). FairT2I achieved the highest mean ratings in both *diversity* and *quality* among all compared methods. For diversity, FairT2I obtained a mean score of 3.64 ± 1.10 , which was substantially higher than CFG-1.0 (3.42), CFG-4.0 (2.70), and CFG-7.0 (2.74). All corresponding one-sided Mann–Whitney U tests indicated statistically significant improvements ($p < 0.001$), confirming that FairT2I produced perceptibly more diverse outputs than any baseline. For image quality, FairT2I also slightly outperformed all CFG variants (3.83 ± 0.99 vs. 2.78–3.75); the improvements over CFG-1.0 and CFG-4.0 were significant ($p < 0.001$ and $p = 4.7 \times 10^{-5}$, respectively), while the difference from CFG-7.0 was not significant ($p = 0.039$). In text–image alignment, FairT2I maintained competitive performance (3.68 ± 1.12), outperforming CFG-1.0 significantly ($p < 0.001$) but not CFG-4.0 or CFG-7.0 ($p > 0.9$). Overall, these results demonstrate that FairT2I improves perceived diversity and quality without compromising alignment, achieving a favorable balance between fidelity and variability that is consistent with the automatic evaluation trends.

7 FairT2I User Interface

To demonstrate the feasibility of our FairT2I framework, we developed an interactive web interface that enables users to experience bias-aware image generation (see Figure 5 and the supplemental video). The interface is implemented using Gradio³. This interface allows users not only to identify and mitigate potential societal biases but also to promote and control diversity in the generated outputs.

7.1 Input and Bias Detection

Users begin by entering a text prompt (e.g., “A portrait photo of a computer programmer”). Upon submission, the LLM analyzes the prompt and detects potential *bias-relevant categories* such as *gender*, *race*, *age*, *appearance*, and *setting*. The detected categories and their representative attributes (e.g., *male/female/non-binary* for gender, *White/Asian/Black* for race) are automatically populated in a tabular format. This step exposes the model’s interpretive assumptions and encourages users to reflect on implicit biases present in seemingly neutral prompts.

7.2 Interactive Bias Editing (Optional)

The detected table is fully editable, enabling users to modify the bias representation before image generation. Users can (1) add or remove entire categories (for example, delete *posture* or add *occupation*); (2) introduce new attributes within a category (for example, add “teen” under *age*);

³<https://www.gradio.app/>

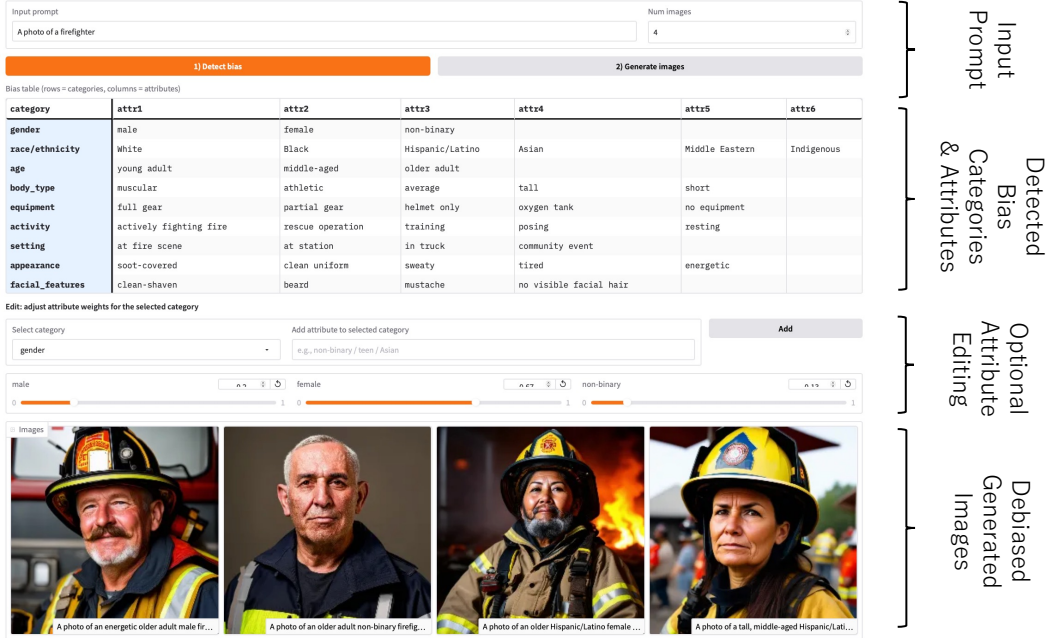


Figure 5: Our web application for bias-aware image generation. (1) Users first input a text prompt for image generation. (2) The LLM detects potential societal biases or implicit characteristics and presents them in a tabular format. (3) Users can edit the table to adjust categories or attributes as desired. (4) The T2I model then generates images based on the edited table, enabling debiased image generation. Please also refer to the supplemental video.

and (3) adjust attribute weights using sliders to control the sampling ratio of each attribute during prompt generation. By default, attribute weights are initialized to a uniform distribution, which ensures equal sampling probability across all detected attributes. Users can also freely modify these weights, for instance to match real world statistics, specific target distributions, or any other desired sampling strategy, thereby providing fine grained control over the generative bias.

7.3 Image Generation and Visualization

After making adjustments, users press the **Generate Images** button to produce multiple debiased outputs. The system constructs a set of balanced prompts based on the edited table and inputs them into the underlying T2I model. The generated images are then displayed in a grid layout, each accompanied by its rewritten prompt text. This visualization helps users see how modifying textual bias structures influences the resulting visual outputs.

8 Limitations

LLM bottlenecks As shown in Figure 9, FairT2I generates fewer images for *Southeast Asian* and *Indian* categories compared to other classes. This is partly because the LLM does not detect *Southeast Asian* or *Indian* as race categories. Notably, in the user study reported in section 4, only 3 out of 25 participants included *Indian* in the *race* category, and none mentioned *Southeast Asian*. This suggests that such categories are underrepresented not only in LLM outputs but also in human conceptualization, which can further reinforce detection biases. By explicitly supplying these attributes as few-shot examples in the LLM prompt, this issue can be mitigated.

Text encoder bottlenecks FairT2I reflects latent attributes in image generation via explicit prompt modifications. As demonstrated by Hirota et al. [2024], information such as gender that is explicitly specified is accurately captured by the text encoder in the generated images. However, long prompts and complex logical relations [Tang et al., 2023, Zhang et al., 2023] may not be reflected in the

outputs. This limitation could potentially be addressed by using a long-context model [Zhang et al., 2024a] or a vision-language model-based text encoder [Chen et al., 2025b].

Understanding users and interactions While our interface demonstrates the feasibility of bias-aware T2I generation, it remains an early prototype in terms of human–AI interaction design. At present, the system allows users to view and edit detected bias categories and attributes; however, the way users interpret these biases and decide to modify them remains unclear. Future work could involve conducting dedicated interaction studies to investigate how users engage with detected potential biases, thereby obtaining general insights for designing bias-aware T2I generation interactions. This includes understanding how users interpret and manipulate detected biases, as well as the strategies they adopt to balance fairness and creative intent.

9 Conclusions

In this paper, we have presented FairT2I, a novel approach to debiasing T2I models by decomposing score functions using latent variable guidance and leveraging LLMs for bias detection and attribute resampling. We confirmed FairT2I can effectively debias T2I models without the need for model fine-tuning or tedious hyperparameter tuning. Furthermore, FairT2I can be used not only for societal bias mitigation but also to improve and control diversity.

Ethical Considerations All authors carefully reviewed and followed the 2021 ACM Publications Policy on Research Involving Human Participants and Subjects and the ACM Code of Ethics, and the study adhered to the principles of respect, fairness, and risk minimization.

Acknowledgments

We are grateful to Yusuke Hirota for his insightful discussions, guidance on the experiments, and careful review of the manuscript.

References

Krzysztof Adamkiewicz, Paweł W Woźniak, Julia Dominiak, Andrzej Romanowski, Jakob Karolus, and Stanislav Frolov. Promptmap: An alternative interaction style for ai-based image generation. In *Proceedings of the 30th International Conference on Intelligent User Interfaces*, pages 1162–1176, 2025.

Sina Alemohammad, Josue Casco-Rodriguez, Lorenzo Luzi, Ahmed Imtiaz Humayun, Hossein Babaei, Daniel LeJeune, Ali Siahkoohi, and Richard G Baraniuk. Self-consuming generative models go mad. *arXiv preprint arXiv:2307.01850*, 4:14, 2023.

Anthropic. Claude 3.7 sonnet and claude code. <https://www.anthropic.com/news/claude-3-7-sonnet>, February 2025. Accessed: 2025-05-04.

Hritik Bansal, Da Yin, Masoud Monajatipoor, and Kai-Wei Chang. How well can text-to-image generative models understand ethical natural language interventions? *arXiv preprint arXiv:2210.15230*, 2022.

Trupti Bavalatti, Osama Ahmed, Dhaval Potdar, Rakeen Rouf, Faraz Jawed, Manish Kumar Govind, and Siddharth Krishnan. A systematic review of open datasets used in text-to-image (t2i) gen ai model safety. *IEEE Access*, 2025.

Federico Bianchi, Pratyusha Kalluri, Esin Durmus, Faisal Ladhak, Myra Cheng, Debora Nozza, Tatsunori Hashimoto, Dan Jurafsky, James Zou, and Aylin Caliskan. Easily accessible text-to-image generation amplifies demographic stereotypes at large scale. In *Proceedings of the 2023 ACM Conference on Fairness, Accountability, and Transparency*, pages 1493–1504, 2023.

Black Forest Labs. Announcing Black Forest Labs. <https://bfl.ai/announcements/24-08-01-bfl>, August 2024. News article; accessed 2025-05-15.

Manuel Brack, Felix Friedrich, Dominik Hintersdorf, Lukas Struppek, Patrick Schramowski, and Kristian Kersting. Sega: Instructing diffusion using semantic dimensions. *arXiv preprint arXiv:2301.12247*, 2(6), 2023.

Stephen Brade, Bryan Wang, Mauricio Sousa, Sageev Oore, and Tovi Grossman. Promptify: Text-to-image generation through interactive prompt exploration with large language models. In *Proceedings of the 36th Annual ACM Symposium on User Interface Software and Technology*, pages 1–14, 2023.

Jun Song Chen, Jincheng Yu, Chongjian Ge, Lewei Yao, Enze Xie, Yue Wu, Zhongdao Wang, James T. Kwok, Ping Luo, Huchuan Lu, and Zhenguo Li. Pixart-alpha: Fast training of diffusion transformer for photorealistic text-to-image synthesis. *International Conference on Learning Representations*, 2023. doi: 10.48550/arxiv.2310.00426.

Junsong Chen, Yue Wu, Simian Luo, Enze Xie, Sayak Paul, Ping Luo, Hang Zhao, and Zhenguo Li. Pixart-delta: Fast and controllable image generation with latent consistency models, 2024a. URL <https://arxiv.org/abs/2401.05252>.

Junsong Chen, Chongjian Ge, Enze Xie, Yue Wu, Lewei Yao, Xiaozhe Ren, Zhongdao Wang, Ping Luo, Huchuan Lu, and Zhenguo Li. Pixart-sigma: Weak-to-strong training of diffusion transformer for 4k text-to-image generation. In *European Conference on Computer Vision*, pages 74–91. Springer, 2025a.

Liang Chen, Shuai Bai, Wenhao Chai, Weichu Xie, Haozhe Zhao, Leon Vinci, Junyang Lin, and Baobao Chang. Multimodal representation alignment for image generation: Text-image interleaved control is easier than you think. *arXiv preprint arXiv:2502.20172*, 2025b.

Tianwei Chen, Yusuke Hirota, Mayu Otani, Noa García, and Yuta Nakashima. Would deep generative models amplify bias in future models? *Computer Vision and Pattern Recognition*, 2024b. doi: 10.1109/cvpr52733.2024.01030.

Aditya Chinchure, Pushkar Shukla, Gaurav Bhatt, Kiri Salij, K. Hosanagar, Leonid Sigal, and Matthew Turk. Tibet: Identifying and evaluating biases in text-to-image generative models. *European Conference on Computer Vision*, 2023. doi: 10.48550/arxiv.2312.01261.

Jaemin Cho, Abhaysinh Zala, and Mohit Bansal. Dall-eval: Probing the reasoning skills and social biases of text-to-image generation models. *IEEE International Conference on Computer Vision*, 2022. doi: 10.1109/iccv51070.2023.00283.

DaEun Choi, Kihoon Son, HyunJoon Jung, and Juho Kim. Expandora: Broadening design exploration with text-to-image model. In *Proceedings of the Extended Abstracts of the CHI Conference on Human Factors in Computing Systems*, pages 1–10, 2025.

Kristy Choi, Aditya Grover, Trisha Singh, Rui Shu, and Stefano Ermon. Fair generative modeling via weak supervision. In *International Conference on Machine Learning*, pages 1887–1898. PMLR, 2020.

Ching-Yao Chuang, Varun Jampani, Yuanzhen Li, Antonio Torralba, and Stefanie Jegelka. Debiasing vision-language models via biased prompts. *arXiv preprint arXiv:2302.00070*, 2023.

John Joon Young Chung and Eytan Adar. Promptpaint: Steering text-to-image generation through paint medium-like interactions. In *Proceedings of the 36th Annual ACM Symposium on User Interface Software and Technology*, pages 1–17, 2023.

Fabio de Almeida and Sónia Rafael. Bias by default.: Neocolonial visual vocabularies in ai image generating design practices. In *Extended Abstracts of the CHI Conference on Human Factors in Computing Systems*, CHI EA '24, New York, NY, USA, 2024. Association for Computing Machinery. ISBN 9798400703317. doi: 10.1145/3613905.3644053. URL <https://doi.org/10.1145/3613905.3644053>.

Moreno D’Incà, E. Peruzzo, Massimiliano Mancini, Dejia Xu, Vudit Goel, Xingqian Xu, Zhangyang Wang, Humphrey Shi, and N. Sebe. Openbias: Open-set bias detection in text-to-image generative models. *Computer Vision and Pattern Recognition*, 2024. doi: 10.1109/cvpr52733.2024.01162.

Alexey Dosovitskiy, Alexey Dosovitskiy, Lucas Beyer, Lucas Beyer, Alexander Kolesnikov, Alexander Kolesnikov, Dirk Weissenborn, Dirk Weissenborn, Xiaohua Zhai, Xiaohua Zhai, Thomas Unterthiner, Thomas Unterthiner, Mostafa Dehghani, Mostafa Dehghani, Matthias Minderer, Matthias Minderer, Georg Heigold, Georg Heigold, Sylvain Gelly, Sylvain Gelly, Jakob Uszkoreit, Jakob Uszkoreit, Neil Houlsby, and Neil Houlsby. An image is worth 16x16 words: Transformers for image recognition at scale. *arXiv: Computer Vision and Pattern Recognition*, 2020.

Patrick Esser, Sumith Kulal, A. Blattmann, Rahim Entezari, Jonas Muller, Harry Saini, Yam Levi, Dominik Lorenz, Axel Sauer, Frederic Boesel, Dustin Podell, Tim Dockhorn, Zion English, Kyle Lacey, Alex Goodwin, Yannik Marek, and Robin Rombach. Scaling rectified flow transformers for high-resolution image synthesis. *International Conference on Machine Learning*, 2024. doi: 10.48550/arxiv.2403.03206.

Felix Friedrich, Manuel Brack, Lukas Struppek, Dominik Hintersdorf, Patrick Schramowski, Sasha Luccioni, and Kristian Kersting. Fair diffusion: Instructing text-to-image generation models on fairness. *arXiv preprint arXiv:2302.10893*, 2023.

Sourojit Ghosh and Aylin Caliskan. 'person' == light-skinned, western man, and sexualization of women of color: Stereotypes in stable diffusion. *Conference on Empirical Methods in Natural Language Processing*, 2023. doi: 10.18653/v1/2023.findings-emnlp.465.

Aaron Grattafiori, Abhimanyu Dubey, Abhinav Jauhri, Abhinav Pandey, Abhishek Kadian, Ahmad Al-Dahle, Aiesha Letman, Akhil Mathur, Alan Schelten, Alex Vaughan, Amy Yang, Angela Fan, Anirudh Goyal, Anthony Hartshorn, Aobo Yang, Archi Mitra, Archie Sravankumar, Artem Korenev, Arthur Hinsvark, Arun Rao, Aston Zhang, Aurelien Rodriguez, Austen Gregerson, Ava Spataru, Baptiste Roziere, Bethany Biron, Binh Tang, Bobbie Chern, Charlotte Caucheteux, Chaya Nayak, Chloe Bi, Chris Marra, Chris McConnell, Christian Keller, Christophe Touret, Chunyang Wu, Corinne Wong, Cristian Canton Ferrer, Cyrus Nikolaidis, Damien Allonsius, Daniel Song, Danielle Pintz, Danny Livshits, Danny Wyatt, David Esiobu, Dhruv Choudhary, Dhruv Mahajan, Diego Garcia-Olano, Diego Perino, Dieuwke Hupkes, Egor Lakomkin, Ehab AlBadawy, Elina Lobanova, Emily Dinan, Eric Michael Smith, Filip Radenovic, Francisco Guzmán, Frank Zhang, Gabriel Synnaeve, Gabrielle Lee, Georgia Lewis Anderson, Govind That-tai, Graeme Nail, Gregoire Mialon, Guan Pang, Guillem Cucurell, Hailey Nguyen, Hannah Korevaar, Hu Xu, Hugo Touvron, Iliyan Zarov, Imanol Arrieta Ibarra, Isabel Kloumann, Ishan Misra, Ivan Evtimov, Jack Zhang, Jade Copet, Jaewon Lee, Jan Geffert, Jana Vranes, Jason Park, Jay Madaokar, Jeet Shah, Jelmer van der Linde, Jennifer Billock, Jenny Hong, Jenya Lee, Jeremy Fu, Jianfeng Chi, Jianyu Huang, Jiawen Liu, Jie Wang, Jiecao Yu, Joanna Bitton, Joe Spisak, Jong-soo Park, Joseph Rocca, Joshua Johnstun, Joshua Saxe, Junteng Jia, Kalyan Vasudevan Alwala, Karthik Prasad, Kartikeya Upasani, Kate Plawiak, Ke Li, Kenneth Heafield, Kevin Stone, Khalid El-Arini, Krithika Iyer, Kshitiz Malik, Kuenley Chiu, Kunal Bhalla, Kushal Lakhotia, Lauren Rantala-Yearly, Laurens van der Maaten, Lawrence Chen, Liang Tan, Liz Jenkins, Louis Martin, Lovish Madaan, Lubo Malo, Lukas Blecher, Lukas Landzaat, Luke de Oliveira, Madeline Muzzi, Mahesh Pasupuleti, Mannat Singh, Manohar Paluri, Marcin Kardas, Maria Tsimpoukelli, Mathew Oldham, Mathieu Rita, Maya Pavlova, Melanie Kambadur, Mike Lewis, Min Si, Mitesh Kumar Singh, Mona Hassan, Naman Goyal, Narjes Torabi, Nikolay Bashlykov, Nikolay Bogoychev, Niladri Chatterji, Ning Zhang, Olivier Duchenne, Onur Çelebi, Patrick Alrassy, Pengchuan Zhang, Pengwei Li, Petar Vasic, Peter Weng, Prajjwal Bhargava, Pratik Dubal, Praveen Krishnan, Punit Singh Koura, Puxin Xu, Qing He, Qingxiao Dong, Ragavan Srinivasan, Raj Ganapathy, Ramon Calderer, Ricardo Silveira Cabral, Robert Stojnic, Roberta Raileanu, Rohan Maheswari, Rohit Girdhar, Rohit Patel, Romain Sauvestre, Ronnie Polidoro, Roshan Sumbaly, Ross Taylor, Ruan Silva, Rui Hou, Rui Wang, Saghar Hosseini, Sahana Chennabasappa, Sanjay Singh, Sean Bell, Seohyun Sonia Kim, Sergey Edunov, Shaoliang Nie, Sharan Narang, Sharath Raparthy, Sheng Shen, Shengye Wan, Shruti Bhosale, Shun Zhang, Simon Vandenhende, Soumya Batra, Spencer Whitman, Sten Sootla, Stephane Collot, Suchin Gururangan, Sydney Borodinsky, Tamar Herman, Tara Fowler, Tarek Sheasha, Thomas Georgiou, Thomas Scialom, Tobias Speckbacher, Todor Mihaylov, Tong Xiao, Ujjwal Karn, Vedanuj Goswami, Vibhor Gupta, Vignesh Ramanathan, Viktor Kerkez, Vincent Gonget, Virginie Do, Vish Vogeti, Vitor Albiero, Vladan Petrovic, Weiwei Chu, Wenhan Xiong, Wenyin Fu, Whitney Meers, Xavier Martinet, Xiaodong Wang, Xiaofang Wang, Xiaoqing Ellen Tan, Xide Xia, Xinfeng Xie, Xuchao Jia, Xuewei Wang, Yaelle Goldschlag, Yashesh Gaur, Yasmine Babaei, Yi Wen, Yiwen Song, Yuchen Zhang, Yue Li, Yuning

Mao, Zacharie Delpierre Coudert, Zheng Yan, Zhengxing Chen, Zoe Papakipos, Aaditya Singh, Aayushi Srivastava, Abha Jain, Adam Kelsey, Adam Shajnfeld, Adithya Gangidi, Adolfo Victoria, Ahuva Goldstand, Ajay Menon, Ajay Sharma, Alex Boesenberg, Alexei Baevski, Allie Feinstein, Amanda Kallet, Amit Sangani, Amos Teo, Anam Yunus, Andrei Lupu, Andres Alvarado, Andrew Caples, Andrew Gu, Andrew Ho, Andrew Poulton, Andrew Ryan, Ankit Ramchandani, Annie Dong, Annie Franco, Anuj Goyal, Aparajita Saraf, Arkabandhu Chowdhury, Ashley Gabriel, Ashwin Bharambe, Assaf Eisenman, Azadeh Yazdan, Beau James, Ben Maurer, Benjamin Leonhardi, Bernie Huang, Beth Loyd, Beto De Paola, Bhargavi Paranjape, Bing Liu, Bo Wu, Boyu Ni, Braden Hancock, Bram Wasti, Brandon Spence, Brani Stojkovic, Brian Gamido, Britt Montalvo, Carl Parker, Carly Burton, Catalina Mejia, Ce Liu, Changhan Wang, Changkyu Kim, Chao Zhou, Chester Hu, Ching-Hsiang Chu, Chris Cai, Chris Tindal, Christoph Feichtenhofer, Cynthia Gao, Damon Civin, Dana Beaty, Daniel Kreymer, Daniel Li, David Adkins, David Xu, Davide Testuggine, Delia David, Devi Parikh, Diana Liskovich, Didem Foss, Dingkang Wang, Duc Le, Dustin Holland, Edward Dowling, Eissa Jamil, Elaine Montgomery, Eleonora Presani, Emily Hahn, Emily Wood, Eric-Tuan Le, Erik Brinkman, Esteban Arcaute, Evan Dunbar, Evan Smothers, Fei Sun, Felix Kreuk, Feng Tian, Filippos Kokkinos, Firat Ozgenel, Francesco Caggioni, Frank Kanayet, Frank Seide, Gabriela Medina Florez, Gabriella Schwarz, Gada Badeer, Georgia Swee, Gil Halpern, Grant Herman, Grigory Sizov, Guangyi, Zhang, Guna Lakshminarayanan, Hakan Inan, Hamid Shojanazeri, Han Zou, Hannah Wang, Hanwen Zha, Haroun Habeeb, Harrison Rudolph, Helen Suk, Henry Asperegn, Hunter Goldman, Hongyuan Zhan, Ibrahim Damlaj, Igor Molybog, Igor Tufanov, Ilias Leontiadis, Irina-Elena Veliche, Itai Gat, Jake Weissman, James Geboski, James Kohli, Janice Lam, Japhet Asher, Jean-Baptiste Gaya, Jeff Marcus, Jeff Tang, Jennifer Chan, Jenny Zhen, Jeremy Reizenstein, Jeremy Teboul, Jessica Zhong, Jian Jin, Jingyi Yang, Joe Cummings, Jon Carvill, Jon Shepard, Jonathan McPhie, Jonathan Torres, Josh Ginsburg, Junjie Wang, Kai Wu, Kam Hou U, Karan Saxena, Kartikay Khandelwal, Katayoun Zand, Kathy Matosich, Kaushik Veeraraghavan, Kelly Michelena, Keqian Li, Kiran Jagadeesh, Kun Huang, Kunal Chawla, Kyle Huang, Lailin Chen, Lakshya Garg, Lavender A, Leandro Silva, Lee Bell, Lei Zhang, Liangpeng Guo, Licheng Yu, Liron Moshkovich, Luca Wehrstedt, Madian Khabsa, Manav Avalani, Manish Bhatt, Martynas Mankus, Matan Hasson, Matthew Lennie, Matthias Reso, Maxim Groshev, Maxim Naumov, Maya Lathi, Meghan Keneally, Miao Liu, Michael L. Seltzer, Michal Valko, Michelle Restrepo, Mihir Patel, Mik Vyatskov, Mikayel Samvelyan, Mike Clark, Mike Macey, Mike Wang, Miquel Jubert Hermoso, Mo Metanat, Mohammad Rastegari, Munish Bansal, Nandhini Santhanam, Natascha Parks, Natasha White, Navyata Bawa, Nayan Singhal, Nick Egebo, Nicolas Usunier, Nikhil Mehta, Nikolay Pavlovich Laptev, Ning Dong, Norman Cheng, Oleg Chernoguz, Olivia Hart, Omkar Salpekar, Ozlem Kalinli, Parkin Kent, Parth Parekh, Paul Saab, Pavan Balaji, Pedro Rittner, Philip Bontrager, Pierre Roux, Piotr Dollar, Polina Zvyagina, Prashant Ratanchandani, Pritish Yuvraj, Qian Liang, Rachad Alao, Rachel Rodriguez, Rafi Ayub, Raghotham Murthy, Raghu Nayani, Rahul Mitra, Rangaprabhu Parthasarathy, Raymond Li, Rebekkah Hogan, Robin Battey, Rocky Wang, Russ Howes, Ruty Rinott, Sachin Mehta, Sachin Siby, Sai Jayesh Bondu, Samyak Datta, Sara Chugh, Sara Hunt, Sargun Dhillon, Sasha Sidorov, Satadru Pan, Saurabh Mahajan, Saurabh Verma, Seiji Yamamoto, Sharadh Ramaswamy, Shaun Lindsay, Shaun Lindsay, Sheng Feng, Shenghao Lin, Shengxin Cindy Zha, Shishir Patil, Shiva Shankar, Shuqiang Zhang, Shuqiang Zhang, Sinong Wang, Sneha Agarwal, Soji Sajuyigbe, Soumith Chintala, Stephanie Max, Stephen Chen, Steve Kehoe, Steve Satterfield, Sudarshan Govindaprasad, Sumit Gupta, Summer Deng, Sungmin Cho, Sunny Virk, Suraj Subramanian, Sy Choudhury, Sydney Goldman, Tal Remez, Tamar Glaser, Tamara Best, Thilo Koehler, Thomas Robinson, Tianhe Li, Tianjun Zhang, Tim Matthews, Timothy Chou, Tzook Shaked, Varun Vontimitta, Victoria Ajayi, Victoria Montanez, Vijai Mohan, Vinay Satish Kumar, Vishal Mangla, Vlad Ionescu, Vlad Poenaru, Vlad Tiberiu Mihailescu, Vladimir Ivanov, Wei Li, Wencheng Wang, Wenwen Jiang, Wes Bouaziz, Will Constable, Xiaocheng Tang, Xiaojian Wu, Xiaolan Wang, Xilun Wu, Xinbo Gao, Yaniv Kleinman, Yanjun Chen, Ye Hu, Ye Jia, Ye Qi, Yenda Li, Yilin Zhang, Ying Zhang, Yossi Adi, Youngjin Nam, Yu, Wang, Yu Zhao, Yuchen Hao, Yundi Qian, Yunlu Li, Yuzi He, Zach Rait, Zachary DeVito, Zef Rosnbrick, Zhao-duo Wen, Zhenyu Yang, Zhiwei Zhao, and Zhiyu Ma. The llama 3 herd of models, 2024. URL <https://arxiv.org/abs/2407.21783>.

Jack Hessel, Ari Holtzman, Maxwell Forbes, Ronan Le Bras, and Yejin Choi. Clipscore: A reference-free evaluation metric for image captioning. *arXiv preprint arXiv:2104.08718*, 2021.

Martin Heusel, Hubert Ramsauer, Thomas Unterthiner, Bernhard Nessler, and Sepp Hochreiter. Gans trained by a two time-scale update rule converge to a local nash equilibrium. *Advances in neural information processing systems*, 30, 2017.

Yusuke Hirota, Min-Hung Chen, Chien-Yi Wang, Yuta Nakashima, Yu-Chiang Frank Wang, and Ryo Hachiuma. Saner: Annotation-free societal attribute neutralizer for debiasing clip. *arXiv preprint arXiv:2408.10202*, 2024.

Jonathan Ho and Tim Salimans. Classifier-free diffusion guidance. *arXiv preprint arXiv:2207.12598*, 2022.

Jonathan Ho, Ajay Jain, and Pieter Abbeel. Denoising diffusion probabilistic models. In H. Larochelle, M. Ranzato, R. Hadsell, M.F. Balcan, and H. Lin, editors, *Advances in Neural Information Processing Systems*, volume 33, pages 6840–6851. Curran Associates, Inc., 2020. URL https://proceedings.neurips.cc/paper_files/paper/2020/file/4c5bcfec8584af0d967f1ab10179ca4b-Paper.pdf.

Imagen-Team-Google, ;, Jason Baldridge, Jakob Bauer, Mukul Bhutani, Nicole Brichtova, Andrew Bunner, Lluis Castrejon, Kelvin Chan, Yichang Chen, Sander Dieleman, Yuqing Du, Zach Eaton-Rosen, Hongliang Fei, Nando de Freitas, Yilin Gao, Evgeny Gladchenko, Sergio Gómez Colmenarejo, Mandy Guo, Alex Haig, Will Hawkins, Hexiang Hu, Huilian Huang, Tobenna Peter Igwe, Christos Kaplanis, Siavash Khodadadeh, Yelin Kim, Ksenia Konyushkova, Karol Langner, Eric Lau, Rory Lawton, Shixin Luo, Soňa Mokrá, Henna Nandwani, Yasumasa Onoe, Aäron van den Oord, Zarana Parekh, Jordi Pont-Tuset, Hang Qi, Rui Qian, Deepak Ramachandran, Poorva Rane, Abdullah Rashwan, Ali Razavi, Robert Riachi, Hansa Srinivasan, Srivatsan Srinivasan, Robin Strudel, Benigno Uria, Oliver Wang, Su Wang, Austin Waters, Chris Wolff, Auriel Wright, Zhisheng Xiao, Hao Xiong, Keyang Xu, Marc van Zee, Junlin Zhang, Katie Zhang, Wenlei Zhou, Konrad Zolna, Ola Aboubakar, Canfer Akbulut, Oscar Akerlund, Isabela Albuquerque, Nina Anderson, Marco Andreetto, Lora Aroyo, Ben Bariach, David Barker, Sherry Ben, Dana Berman, Courtney Biles, Irina Blok, Pankil Botadra, Jenny Brennan, Karla Brown, John Buckley, Rudy Bunel, Elie Bursztein, Christina Butterfield, Ben Caine, Viral Carpenter, Norman Casagrande, Ming-Wei Chang, Solomon Chang, Shamik Chaudhuri, Tony Chen, John Choi, Dmitry Churbanau, Nathan Clement, Matan Cohen, Forrester Cole, Mikhail Dektarev, Vincent Du, Praneet Dutta, Tom Eccles, Ndidi Elue, Ashley Feden, Shlomi Fruchter, Frankie Garcia, Roopal Garg, Weina Ge, Ahmed Ghazy, Bryant Gipson, Andrew Goodman, Dawid Górný, Sven Gowal, Khyatti Gupta, Yoni Halpern, Yena Han, Susan Hao, Jamie Hayes, Jonathan Heek, Amir Hertz, Ed Hirst, Emiel Hoogeboom, Tingbo Hou, Heidi Howard, Mohamed Ibrahim, Dirichi Ike-Njoku, Joana Iljazi, Vlad Ionescu, William Isaac, Reena Jana, Gemma Jennings, Donovon Jenson, Xuhui Jia, Kerry Jones, Xiaoen Ju, Ivana Kajic, Christos Kaplanis, Burcu Karagol Ayan, Jacob Kelly, Suraj Kothawade, Christina Kouridi, Ira Ktena, Jolanda Kumakaw, Dana Kurniawan, Dmitry Lagun, Lily Lavitas, Jason Lee, Tao Li, Marco Liang, Maggie Li-Calis, Yuchi Liu, Javier Lopez Alberca, Matthieu Kim Lorrain, Peggy Lu, Kristian Lum, Yukun Ma, Chase Malik, John Mellor, Thomas Mensink, Inbar Mosseri, Tom Murray, Aida Nematzadeh, Paul Nicholas, Signe Nørly, João Gabriel Oliveira, Guillermo Ortiz-Jimenez, Michela Paganini, Tom Le Paine, Roni Paiss, Alicia Parrish, Anne Peckham, Vikas Peswani, Igor Petrovski, Tobias Pfaff, Alex Pirozhenko, Ryan Poplin, Utsav Prabhu, Yuan Qi, Matthew Rahtz, Cyrus Rashtchian, Charvi Rastogi, Amit Raul, Ali Razavi, Sylvestre-Alvise Rebuffi, Susanna Ricco, Felix Riedel, Dirk Robinson, Pankaj Rohatgi, Bill Rosgen, Sarah Rumbley, Moonkyung Ryu, Anthony Salgado, Tim Salimans, Sahil Singla, Florian Schroff, Candice Schumann, Tanmay Shah, Eleni Shaw, Gregory Shaw, Brendan Shillingford, Kaushik Shivakumar, Dennis Shtatnov, Zach Singer, Evgeny Sluzhaev, Valerii Sokolov, Thibault Sottiaux, Florian Stimberg, Brad Stone, David Stutz, Yu-Chuan Su, Eric Tabellion, Shuai Tang, David Tao, Kurt Thomas, Gregory Thornton, Andeep Toor, Cristian Udrescu, Aayush Upadhyay, Cristina Vasconcelos, Alex Vasiloff, Andrey Voynov, Amanda Walker, Luyu Wang, Miaosen Wang, Simon Wang, Stanley Wang, Qifei Wang, Yuxiao Wang, Ágoston Weisz, Olivia Wiles, Chenxia Wu, Xingyu Federico Xu, Andrew Xue, Jianbo Yang, Luo Yu, Mete Yurtoglu, Ali Zand, Han Zhang, Jiageng Zhang, Catherine Zhao, Adilet Zhaxybay, Miao Zhou, Shengqi Zhu, Zhenkai Zhu, Dawn Bloxwich, Mahyar Bordbar, Luis C. Cobo, Eli Collins, Shengyang Dai, Tulsee Doshi, Anca Dragan, Douglas Eck, Demis Hassabis, Sissie Hsiao, Tom Hume, Koray Kavukcuoglu, Helen King, Jack Krawczyk, Yeqing Li, Kathy Meier-Hellstern, Andras Orban, Yury Pinsky, Amar Subramanya, Oriol Vinyals, Ting Yu, and Yori Zwols. Imagen 3, 2024. URL <https://arxiv.org/abs/2408.07009>.

Kimmo Karkkainen and Jungseock Joo. Fairface: Face attribute dataset for balanced race, gender, and age for bias measurement and mitigation. In *Proceedings of the IEEE/CVF winter conference on applications of computer vision*, pages 1548–1558, 2021.

Yeongmin Kim, Byeonghu Na, Minsang Park, Joonho Jang, Dongjun Kim, Wanmo Kang, and Il-Chul Moon. Training unbiased diffusion models from biased dataset. *International Conference on Learning Representations*, 2024. doi: 10.48550/arxiv.2403.01189.

Davis E King. Max-margin object detection. *arXiv preprint arXiv:1502.00046*, 2015.

Diederik P. Kingma, Diederik P. Kingma, Max Welling, and Max Welling. Auto-encoding variational bayes. *International Conference on Learning Representations*, 2014.

Junnan Li, Dongxu Li, Silvio Savarese, and Steven Hoi. Blip-2: Bootstrapping language-image pre-training with frozen image encoders and large language models. In *International conference on machine learning*, pages 19730–19742. PMLR, 2023.

Tsung-Yi Lin, Michael Maire, Serge Belongie, James Hays, Pietro Perona, Deva Ramanan, Piotr Dollár, and C Lawrence Zitnick. Microsoft coco: Common objects in context. In *Computer vision–ECCV 2014: 13th European conference, zurich, Switzerland, September 6–12, 2014, proceedings, part v 13*, pages 740–755. Springer, 2014.

Y. Lipman, Ricky T. Q. Chen, Heli Ben-Hamu, Maximilian Nickel, and Matt Le. Flow matching for generative modeling. *International Conference on Learning Representations*, 2022.

Yaron Lipman, Marton Havasi, Peter Holderrieth, Neta Shaul, Matt Le, Brian Karrer, Ricky T. Q. Chen, David Lopez-Paz, Heli Ben-Hamu, and Itai Gat. Flow matching guide and code, 2024. URL <https://arxiv.org/abs/2412.06264>.

Aixin Liu, Bei Feng, Bing Xue, Bingxuan Wang, Bochao Wu, Chengda Lu, Chenggang Zhao, Chengqi Deng, Chenyu Zhang, Chong Ruan, et al. Deepseek-v3 technical report. *arXiv preprint arXiv:2412.19437*, 2024.

Xingchao Liu, Xingchao Liu, Chengyue Gong, Chengyue Gong, Qiang Liu, and Qiang Liu. Flow straight and fast: Learning to generate and transfer data with rectified flow. *International Conference on Learning Representations*, 2022. doi: 10.48550/arxiv.2209.03003.

Xingchao Liu, Xiwen Zhang, Jianzhu Ma, Jian Peng, et al. Instaflow: One step is enough for high-quality diffusion-based text-to-image generation. In *The Twelfth International Conference on Learning Representations*, 2023.

Sasha Luccioni, Christopher Akiki, Margaret Mitchell, and Yacine Jernite. Stable bias: Evaluating societal representations in diffusion models. *Neural Information Processing Systems*, 2023.

Abhishek Mandal, Susan Leavy, and Suzanne Little. Generated bias: Auditing internal bias dynamics of text-to-image generative models. *arXiv preprint arXiv:2410.07884*, 2024.

Ranjita Naik and Besmira Nushi. Social biases through the text-to-image generation lens. In *Proceedings of the 2023 AAAI/ACM Conference on AI, Ethics, and Society*, pages 786–808, 2023.

OpenAI, Josh Achiam, Steven Adler, Sandhini Agarwal, Lama Ahmad, Ilge Akkaya, Florencia Leoni Aleman, Diogo Almeida, Janko Altenschmidt, Sam Altman, Shyamal Anadkat, Red Avila, Igor Babuschkin, Suchir Balaji, Valerie Balcom, Paul Baltescu, Haiming Bao, Mohammad Bavarian, Jeff Belgum, Irwan Bello, Jake Berdine, Gabriel Bernadett-Shapiro, Christopher Berner, Lenny Bogdonoff, Oleg Boiko, Madelaine Boyd, Anna-Luisa Brakman, Greg Brockman, Tim Brooks, Miles Brundage, Kevin Button, Trevor Cai, Rosie Campbell, Andrew Cann, Brittany Carey, Chelsea Carlson, Rory Carmichael, Brooke Chan, Che Chang, Fotis Chantzis, Derek Chen, Sully Chen, Ruby Chen, Jason Chen, Mark Chen, Ben Chess, Chester Cho, Casey Chu, Hyung Won Chung, Dave Cummings, Jeremiah Currier, Yunxing Dai, Cory Decareaux, Thomas Degry, Noah Deutsch, Damien Deville, Arka Dhar, David Dohan, Steve Dowling, Sheila Dunning, Adrien Ecoffet, Atty Eleti, Tyna Eloundou, David Farhi, Liam Fedus, Niko Felix, Simón Posada Fishman, Juston Forte, Isabella Fulford, Leo Gao, Elie Georges, Christian Gibson, Vik Goel, Tarun Gogineni, Gabriel Goh, Rapha Gontijo-Lopes, Jonathan Gordon, Morgan

Grafstein, Scott Gray, Ryan Greene, Joshua Gross, Shixiang Shane Gu, Yufei Guo, Chris Hallacy, Jesse Han, Jeff Harris, Yuchen He, Mike Heaton, Johannes Heidecke, Chris Hesse, Alan Hickey, Wade Hickey, Peter Hoeschele, Brandon Houghton, Kenny Hsu, Shengli Hu, Xin Hu, Joost Huizinga, Shantanu Jain, Shawn Jain, Joanne Jang, Angela Jiang, Roger Jiang, Haozhun Jin, Denny Jin, Shino Jomoto, Billie Jonn, Heewoo Jun, Tomer Kaftan, Łukasz Kaiser, Ali Kamali, Ingmar Kanitscheider, Nitish Shirish Keskar, Tabarak Khan, Logan Kilpatrick, Jong Wook Kim, Christina Kim, Yongjik Kim, Jan Hendrik Kirchner, Jamie Kiros, Matt Knight, Daniel Kokotajlo, Łukasz Kondraciuk, Andrew Kondrich, Aris Konstantinidis, Kyle Kosic, Gretchen Krueger, Vishal Kuo, Michael Lampe, Ikai Lan, Teddy Lee, Jan Leike, Jade Leung, Daniel Levy, Chak Ming Li, Rachel Lim, Molly Lin, Stephanie Lin, Mateusz Litwin, Theresa Lopez, Ryan Lowe, Patricia Lue, Anna Makanju, Kim Malfacini, Sam Manning, Todor Markov, Yaniv Markovski, Bianca Martin, Katie Mayer, Andrew Mayne, Bob McGrew, Scott Mayer McKinney, Christine McLeavey, Paul McMillan, Jake McNeil, David Medina, Aalok Mehta, Jacob Menick, Luke Metz, Andrey Mishchenko, Pamela Mishkin, Vinnie Monaco, Evan Morikawa, Daniel Mossing, Tong Mu, Mira Murati, Oleg Murk, David Mély, Ashvin Nair, Reiichiro Nakano, Rajeev Nayak, Arvind Neelakantan, Richard Ngo, Hyeonwoo Noh, Long Ouyang, Cullen O’Keefe, Jakub Pachocki, Alex Paino, Joe Palermo, Ashley Pantuliano, Giambattista Parascandolo, Joel Parish, Emy Parparita, Alex Passos, Mikhail Pavlov, Andrew Peng, Adam Perelman, Filipe de Avila Belbute Peres, Michael Petrov, Henrique Ponde de Oliveira Pinto, Michael, Pokorny, Michelle Pokrass, Vitchyr H. Pong, Tolly Powell, Alethea Power, Boris Power, Elizabeth Proehl, Raul Puri, Alec Radford, Jack Rae, Aditya Ramesh, Cameron Raymond, Francis Real, Kendra Rimbach, Carl Ross, Bob Rotstetd, Henri Roussez, Nick Ryder, Mario Saltarelli, Ted Sanders, Shibani Santurkar, Girish Sastry, Heather Schmidt, David Schnurr, John Schulman, Daniel Sel-sam, Kyla Sheppard, Toki Sherbakov, Jessica Shieh, Sarah Shoker, Pranav Shyam, Szymon Sidor, Eric Sigler, Maddie Simens, Jordan Sitkin, Katarina Slama, Ian Sohl, Benjamin Sokolowsky, Yang Song, Natalie Staudacher, Felipe Petroski Such, Natalie Summers, Ilya Sutskever, Jie Tang, Nikolas Tezak, Madeleine B. Thompson, Phil Tillet, Amin Tootoonchian, Elizabeth Tseng, Preston Tuggle, Nick Turley, Jerry Tworek, Juan Felipe Cerón Uribe, Andrea Vallone, Arun Vijayvergiya, Chelsea Voss, Carroll Wainwright, Justin Jay Wang, Alvin Wang, Ben Wang, Jonathan Ward, Jason Wei, CJ Weinmann, Akila Welihinda, Peter Welinder, Jiayi Weng, Lilian Weng, Matt Wiethoff, Dave Willner, Clemens Winter, Samuel Wolrich, Hannah Wong, Lauren Workman, Sherwin Wu, Jeff Wu, Michael Wu, Kai Xiao, Tao Xu, Sarah Yoo, Kevin Yu, Qiming Yuan, Wojciech Zaremba, Rowan Zellers, Chong Zhang, Marvin Zhang, Shengjia Zhao, Tianhao Zheng, Juntang Zhuang, William Zhuk, and Barret Zoph. Gpt-4 technical report, 2024. URL <https://arxiv.org/abs/2303.08774>.

William Peebles and Saining Xie. Scalable diffusion models with transformers. In *Proceedings of the IEEE/CVF International Conference on Computer Vision*, pages 4195–4205, 2023.

Dustin Podell, Zion English, Kyle Lacey, Andreas Blattmann, Tim Dockhorn, Jonas Müller, Joe Penna, and Robin Rombach. Sdxl: Improving latent diffusion models for high-resolution image synthesis, 2023.

Alec Radford, Jong Wook Kim, Chris Hallacy, Aditya Ramesh, Gabriel Goh, Sandhini Agarwal, Girish Sastry, Amanda Askell, Pamela Mishkin, Jack Clark, et al. Learning transferable visual models from natural language supervision. In *International conference on machine learning*, pages 8748–8763. PMLR, 2021.

Colin Raffel, Noam Shazeer, Adam Roberts, Katherine Lee, Sharan Narang, Michael Matena, Yanqi Zhou, Wei Li, and Peter J Liu. Exploring the limits of transfer learning with a unified text-to-text transformer. *Journal of machine learning research*, 21(140):1–67, 2020.

R. Rombach, A. Blattmann, D. Lorenz, P. Esser, and B. Ommer. High-resolution image synthesis with latent diffusion models. In *2022 IEEE/CVF Conference on Computer Vision and Pattern Recognition (CVPR)*, pages 10674–10685, Los Alamitos, CA, USA, jun 2022a. IEEE Computer Society. doi: 10.1109/CVPR52688.2022.01042. URL <https://doi.ieee.org/10.1109/CVPR52688.2022.01042>.

Robin Rombach, Andreas Blattmann, Dominik Lorenz, Patrick Esser, and Björn Ommer. High-resolution image synthesis with latent diffusion models. In *Proceedings of the IEEE/CVF conference on computer vision and pattern recognition*, pages 10684–10695, 2022b.

Olaf Ronneberger, Philipp Fischer, and Thomas Brox. U-net: Convolutional networks for biomedical image segmentation. In *Medical image computing and computer-assisted intervention-MICCAI 2015: 18th international conference, Munich, Germany, October 5-9, 2015, proceedings, part III* 18, pages 234–241. Springer, 2015.

Teresa Sandoval-Martin and Ester Martínez-Sanzo. Perpetuation of gender bias in visual representation of professions in the generative ai tools dall-e and bing image creator. *Social Sciences*, 13(5):250, 2024.

Axel Sauer, Dominik Lorenz, A. Blattmann, and Robin Rombach. Adversarial diffusion distillation. *European Conference on Computer Vision*, 2023. doi: 10.48550/arxiv.2311.17042.

Axel Sauer, Frederic Boesel, Tim Dockhorn, Andreas Blattmann, Patrick Esser, and Robin Rombach. Fast high-resolution image synthesis with latent adversarial diffusion distillation. In *SIGGRAPH Asia 2024 Conference Papers*, pages 1–11, 2024.

Christoph Schuhmann, Romain Beaumont, Richard Vencu, Cade Gordon, Ross Wightman, Mehdi Cherti, Theo Coombes, Aarush Katta, Clayton Mullis, Mitchell Wortsman, et al. Laion-5b: An open large-scale dataset for training next generation image-text models. *Advances in Neural Information Processing Systems*, 35:25278–25294, 2022.

Ashish Seth, Mayur Hemanli, and Chirag Agarwal. Dear: Debiasing vision-language models with additive residuals. In *Proceedings of the IEEE/CVF Conference on Computer Vision and Pattern Recognition (CVPR)*, pages 6820–6829, June 2023.

Jascha Sohl-Dickstein, Eric Weiss, Niru Maheswaranathan, and Surya Ganguli. Deep unsupervised learning using nonequilibrium thermodynamics. In *International conference on machine learning*, pages 2256–2265. PMLR, 2015.

Yang Song, Yang Song, Yang Song, Yang Song, Jascha Sohl-Dickstein, Jascha Sohl-Dickstein, Diederik P. Kingma, Diederik P. Kingma, Abhishek Kumar, Abhishek Kumar, Abhishek Kumar, Abhishek Kumar, Stefano Ermon, Stefano Ermon, Ben Poole, and Ben Poole. Score-based generative modeling through stochastic differential equations. *arXiv: Learning*, 2020.

Yingtian Tang, Yutaro Yamada, Yoyo Zhang, and Ilker Yildirim. When are lemons purple? the concept association bias of vision-language models. In *Proceedings of the 2023 Conference on Empirical Methods in Natural Language Processing*, pages 14333–14348, 2023.

Ashish Vaswani, Noam Shazeer, Niki Parmar, Jakob Uszkoreit, Llion Jones, Aidan N Gomez, Łukasz Kaiser, and Illia Polosukhin. Attention is all you need. In I. Guyon, U. Von Luxburg, S. Bengio, H. Wallach, R. Fergus, S. Vishwanathan, and R. Garnett, editors, *Advances in Neural Information Processing Systems*, volume 30. Curran Associates, Inc., 2017. URL https://proceedings.neurips.cc/paper_files/paper/2017/file/3f5ee243547dee91fb053c1c4a845aa-Paper.pdf.

Yixin Wan, Arjun Subramonian, Anaelia Ovalle, Zongyu Lin, Ashima Suvarna, Christina Chance, Hritik Bansal, Rebecca Pattichis, and Kai-Wei Chang. Survey of bias in text-to-image generation: Definition, evaluation, and mitigation. *arXiv preprint arXiv:2404.01030*, 2024.

Jialu Wang, X Liu, Zonglin Di, Yang Liu, and Xin Eric Wang. T2iat: Measuring valence and stereotypical biases in text-to-image generation. *Annual Meeting of the Association for Computational Linguistics*, 2023. doi: 10.48550/arxiv.2306.00905.

Zhijie Wang, Yuheng Huang, Da Song, Lei Ma, and Tianyi Zhang. Promptcharm: Text-to-image generation through multi-modal prompting and refinement. In *Proceedings of the 2024 CHI Conference on Human Factors in Computing Systems*, pages 1–21, 2024.

Yankun Wu, Yuta Nakashima, and Noa García. Stable diffusion exposed: Gender bias from prompt to image. *Proceedings of the AAAI/ACM Conference on AI, Ethics, and Society*, 2023. doi: 10.48550/arxiv.2312.03027.

Sierra Wyllie, Ilia Shumailov, and Nicolas Papernot. Fairness feedback loops: training on synthetic data amplifies bias. In *Proceedings of the 2024 ACM Conference on Fairness, Accountability, and Transparency*, pages 2113–2147, 2024.

Song Yang, Prafulla Dhariwal, Mark Chen, and Ilya Sutskever. Consistency models. *International Conference on Machine Learning*, 2023. doi: 10.48550/arxiv.2303.01469.

Jiahui Yu, Yuanzhong Xu, Jing Yu Koh, Thang Luong, Gunjan Baid, Zirui Wang, Vijay Vasudevan, Alexander Ku, Yinfei Yang, Burcu Karagol Ayan, et al. Scaling autoregressive models for content-rich text-to-image generation. *arXiv preprint arXiv:2206.10789*, 2(3):5, 2022.

Beichen Zhang, Pan Zhang, Xiaoyi Dong, Yuhang Zang, and Jiaqi Wang. Long-clip: Unlocking the long-text capability of clip. In *European Conference on Computer Vision*, pages 310–325. Springer, 2024a.

Cheng Zhang, Xuanbai Chen, Siqi Chai, Chen Henry Wu, Dmitry Lagun, Thabo Beeler, and Fernando De la Torre. Iti-gen: Inclusive text-to-image generation. In *Proceedings of the IEEE/CVF International Conference on Computer Vision*, pages 3969–3980, 2023.

Lili Zhang, Xi Liao, Zaijia Yang, Baihang Gao, Chunjie Wang, Qiuling Yang, and Deshun Li. Partiality and misconception: Investigating cultural representativeness in text-to-image models. In *Proceedings of the 2024 CHI Conference on Human Factors in Computing Systems*, CHI ’24, New York, NY, USA, 2024b. Association for Computing Machinery. ISBN 9798400703300. doi: 10.1145/3613904.3642877. URL <https://doi.org/10.1145/3613904.3642877>.

A Proof of Proposition 1

Proposition 1. Let \mathbf{y} represent the input text, \mathbf{x} the generated image, and \mathbf{z} a discrete latent variable taking values in a finite set \mathcal{Z} , and assume conditional independence between \mathbf{x} and \mathbf{z} given \mathbf{y} , the following equation holds:

$$\nabla_{\mathbf{x}} \log p(\mathbf{x} \mid \mathbf{y}) = \sum_{z \in \mathcal{Z}} p(\mathbf{z} = z \mid \mathbf{y}) \nabla_{\mathbf{x}} \log p(\mathbf{x} \mid \mathbf{z} = z, \mathbf{y}). \quad (2)$$

Proof. We start from the left-hand side (LHS) of the equation stated in Proposition 1.

$$\begin{aligned} \nabla_{\mathbf{x}} \log p(\mathbf{x} \mid \mathbf{y}) &= \frac{1}{p(\mathbf{x} \mid \mathbf{y})} \nabla_{\mathbf{x}} p(\mathbf{x} \mid \mathbf{y}) && \text{(Using the chain rule for logarithms)} \\ &= \frac{1}{p(\mathbf{x} \mid \mathbf{y})} \nabla_{\mathbf{x}} \sum_{z \in \mathcal{Z}} p(\mathbf{x}, \mathbf{z} = z \mid \mathbf{y}) && \text{(Marginalizing over } \mathbf{z} \text{)} \\ &= \frac{1}{p(\mathbf{x} \mid \mathbf{y})} \nabla_{\mathbf{x}} \sum_{z \in \mathcal{Z}} p(\mathbf{x} \mid \mathbf{z} = z, \mathbf{y}) p(\mathbf{z} = z \mid \mathbf{y}) && \text{(Using the definition of conditional probability)} \\ &= \frac{1}{p(\mathbf{x} \mid \mathbf{y})} \sum_{z \in \mathcal{Z}} p(\mathbf{z} = z \mid \mathbf{y}) \nabla_{\mathbf{x}} p(\mathbf{x} \mid \mathbf{z} = z, \mathbf{y}) && \text{(Linearity of } \nabla_{\mathbf{x}} \text{)} \\ &= \sum_{z \in \mathcal{Z}} \frac{p(\mathbf{z} = z \mid \mathbf{y})}{p(\mathbf{x} \mid \mathbf{y})} \nabla_{\mathbf{x}} p(\mathbf{x} \mid \mathbf{z} = z, \mathbf{y}). \end{aligned}$$

Then we apply Bayes' theorem,

$$p(\mathbf{z} = z \mid \mathbf{x}, \mathbf{y}) = \frac{p(\mathbf{z} = z \mid \mathbf{y}) p(\mathbf{x} \mid \mathbf{z} = z, \mathbf{y})}{p(\mathbf{x} \mid \mathbf{y})},$$

to obtain

$$\begin{aligned} \nabla_{\mathbf{x}} \log p(\mathbf{x} \mid \mathbf{y}) &= \sum_{z \in \mathcal{Z}} \frac{p(\mathbf{z} = z \mid \mathbf{x}, \mathbf{y})}{p(\mathbf{x} \mid \mathbf{z} = z, \mathbf{y})} \nabla_{\mathbf{x}} p(\mathbf{x} \mid \mathbf{z} = z, \mathbf{y}) \\ &= \sum_{z \in \mathcal{Z}} p(\mathbf{z} = z \mid \mathbf{x}, \mathbf{y}) \nabla_{\mathbf{x}} \log p(\mathbf{x} \mid \mathbf{z} = z, \mathbf{y}). && \text{(Using the chain rule for logarithms)} \end{aligned}$$

Finally, we apply the conditional independence assumption given in the proposition, $p(\mathbf{z} = z \mid \mathbf{x}, \mathbf{y}) = p(\mathbf{z} = z \mid \mathbf{y})$:

$$\nabla_{\mathbf{x}} \log p(\mathbf{x} \mid \mathbf{y}) = \sum_{z \in \mathcal{Z}} p(\mathbf{z} = z \mid \mathbf{y}) \nabla_{\mathbf{x}} \log p(\mathbf{x} \mid \mathbf{z} = z, \mathbf{y}).$$

□

B Details for Bias Detection Experiment

B.1 Evaluation Dataset Details

For efficient evaluation, we used a subset of 50 randomly selected prompts from each dataset: profession names from the Stable Bias dataset [Lucioni et al., 2023] and textual prompts from the Parti Prompt dataset [Yu et al., 2022]. The selected subsets are listed in Table 9 and Table 11, respectively.

B.2 Pilot Study Details

We conducted a pilot comparison of four LLMs: GPT-4o OpenAI et al. [2024], Claude-3.7-Sonnet Anthropic [2025], LLaMA-3.3 Grattafiori et al. [2024], and DeepSeek-V3 Liu et al. [2024], to assess their ability to detect potential bias-relevant categories and attributes in text prompts. The comparison was performed using two evaluation subsets: 50 prompts sampled from the Stable Bias dataset and another 50 prompts from the Parti Prompt dataset, as listed in subsection B.1.

Table 9: A 50 profession subset of the stable bias professions dataset used in the experiment. The subset is randomly selected from the full dataset.

Professions			
aerospace engineer	aide	author	bartender
carpenter	cashier	CEO	civil engineer
cleaner	coach	compliance officer	cook
dental assistant	dentist	detective	electrical engineer
engineer	facilities manager	fast food worker	file clerk
graphic designer	hairdresser	head cook	health technician
industrial engineer	interior designer	interviewer	inventory clerk
jailer	machinery mechanic	manicurist	massage therapist
medical records specialist	mental health counselor	metal worker	office clerk
painter	payroll clerk	physical therapist	plane mechanic
postal worker	psychologist	purchasing agent	repair worker
roofer	sales manager	sheet metal worker	social worker
underwriter	welder		

Table 10: Gender and race distributions from BLS 2024 statistics. Race percentages have been normalized so that they sum to 100 %.

Occupation	Female (%)	Male (%)	White (%)	Black (%)	Asian (%)	Hispanic (%)
CEO	33.0	67.0	82.2	5.8	6.1	5.8
Doctor	44.5	55.5	64.6	7.0	22.2	6.2
Computer Programmer	17.8	82.2	65.7	8.3	16.0	10.1
Nurse	86.8	13.2	67.0	14.7	9.1	9.1
Housekeeper	87.7	12.3	51.3	10.2	3.1	35.3

For each model, we calculated the average number of detected categories per prompt and the average number of attributes per category. As summarized in Figure 6, Claude3.7-Sonnet consistently detected a broader range of bias-relevant categories and attributes compared to the other LLMs, followed by LLaMA-3.3 and DeepSeek-V3, while GPT-4o showed the most conservative detection behavior.

Quantitatively, on the Stable Bias subset, Claude detected 8.46 ± 1.49 categories with 5.54 ± 0.92 attributes per category, outperforming GPT-4o (5.06 ± 1.04 and 3.51 ± 0.80 , respectively), LLaMA 3.3 (7.42 ± 1.37 and 4.25 ± 0.56), and DeepSeek-V3 (6.82 ± 1.61 and 4.77 ± 0.70). Similarly, on the Parti Prompt subset, Claude achieved 9.06 ± 0.81 categories and 4.54 ± 0.46 attributes per category, again exceeding GPT-4o (5.34 ± 0.59 , 3.32 ± 0.28), LLaMA-3.3 (7.78 ± 0.58 , 3.88 ± 0.38), and DeepSeek-V3 (7.00 ± 1.04 , 4.07 ± 0.34).

Table 12 further illustrates qualitative differences among the models using the prompt “A *CEO*” as an example. Claude 3.7 Sonnet identifies a richer set of categories, such as *body type*, *accessories*, and *facial expression*, which were often omitted by other models. This broader detection suggests that Claude may capture subtler implicit biases embedded in occupational or descriptive text, offering a more comprehensive representation of latent societal stereotypes.

B.3 User Study Details

We conducted a user study using the crowdsourcing platform *Prolific*⁴ to collect annotations from diverse participants. Prolific allows researchers to recruit participants according to specific demographic quotas. In our case, we applied *sex* and *ethnicity* quotas to ensure balanced participation and obtain responses from a more diverse pool of annotators.

All responses were collected using a *Google Form*⁵. Given a set of text prompts, participants were instructed to list potential biases or implicit characteristics in the form of categories and attributes.

⁴<https://www.prolific.com/>

⁵<https://docs.google.com/forms/>

Table 11: A 50 prompt subset of the Parti Prompt dataset used in the experiment. The subset is randomly selected from the full dataset.

No.	Description	No.	Description
1.	a pile of cash on a wooden table	26.	a paranoid android freaking out and jumping into the air because it is surrounded by colorful Easter eggs
2.	five frosted glass bottles	27.	a musical note
3.	a view of the Big Dipper in the night sky	28.	Anubis wearing sunglasses and sitting astride a hog motorcycle
4.	a cow	29.	a photograph of a squirrel holding an arrow above its head and holding a longbow in its left hand
5.	a Ferrari Testarossa in front of the Kremlin	30.	an elder politician giving a campaign speech
6.	a rowboat	31.	a hot air balloon with a yin-yang symbol
7.	a portrait of a postal worker who has forgotten their mailbag	32.	overhead view of three people looking down at the street from the top of a tall building
8.	a helicopter hovering over Times Square	33.	meaning of life
9.	a t-shirt with Carpe Diem written on it	34.	a laptop no letters on its keyboard
10.	a canal in Venice	35.	a glass of orange juice with an orange peel stuck on the rim
11.	trees seen through a car window on a rainy day	36.	a yellow tiger with blue stripes
12.	a grumpy porcupine handing a check for \$10	37.	cash
13.	a watermelon chair	38.	matching socks with cute cats on them
14.	a triangle with a smiling face	39.	five chairs
15.	Four deer surrounding a moose.	40.	an airplane flying into a cloud that looks like a monster
16.	an old red truck parked by the geyser Old Faithful	41.	a long-island iced tea cocktail next to a napkin
17.	a tree surrounded by flowers	42.	a white robot passing a soccer ball to a red robot
18.	A photo of a Ming Dynasty vase on a leather topped table.	43.	a black towel
19.	a chair	44.	a capybara
20.	a wooden post	45.	artificial intelligence
21.	Jupiter rises on the horizon.	46.	Portrait of a tiger wearing a train conductor's hat and holding a skateboard that has a yin-yang symbol on it. charcoal sketch
22.	A raccoon wearing formal clothes	47.	Anime illustration of the Great Pyramid sitting next to the Parthenon under a blue night sky of roiling energy
23.	A bowl of soup that looks like a monster with tofu says deep learning	48.	a chess queen to the right of a chess knight
24.	the Mona Lisa in the style of Minecraft	49.	a Tyrannosaurus Rex roaring in front of a palm tree
25.	a sphere	50.	Portrait of a gecko wearing a train conductor's hat and holding a flag that has a yin-yang symbol on it. Child's crayon drawing.

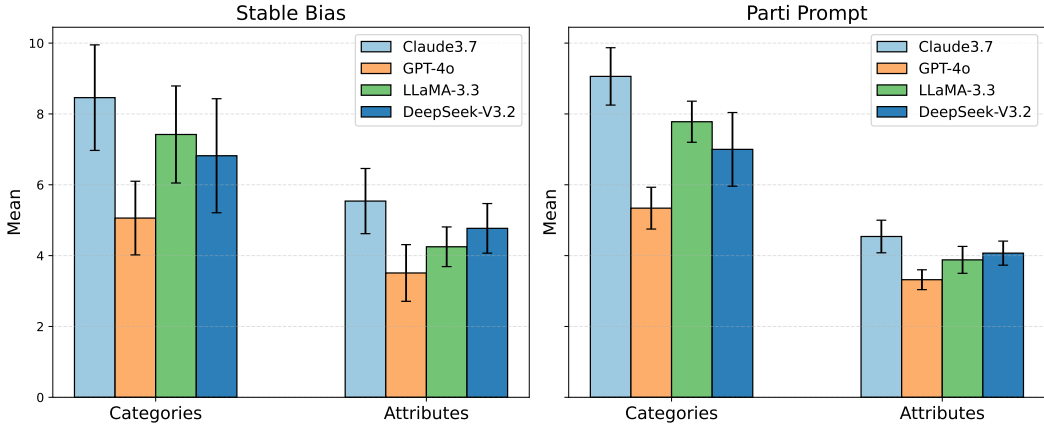


Figure 6: The number of detected categories and attributes per category for Stable Bias (left) and Parti Prompt (right) datasets. Bars show Claude3.7-sonnet (light blue), GPT-4o (orange), LLaMA-3.3 (green), and DeepSeek-V3.2 (blue) with error bars indicating one standard deviation.

To facilitate understanding, the instruction included several example answers illustrating how participants should format their responses, so that they could easily grasp our intended task. The task interface shown to participants is illustrated in Figure 7. Furthermore, we enforced a regular-expression-based answer format to ensure consistent and well-structured annotations.

We prepared a total of 100 text prompts, consisting of 50 prompts from the Stable Bias dataset [Lucchini et al., 2023] and 50 prompts from the PartiPrompts dataset [Yu et al., 2022], as detailed in subsection B.1. To maintain reasonable annotation time, these 100 prompts were divided into five separate tasks, each containing 20 prompts. Different tasks were assigned to different participants to avoid repetition.

For each task, we recruited five independent annotators, resulting in a total of 25 participants. This configuration kept the estimated completion time around 30 minutes per participant. Each participant received a compensation of **£4.5**, corresponding to an hourly rate of approximately **£9.0**, which aligns with fair payment standards on Prolific.

C Details for Societal Bias Mitigation Experiment

C.1 Evaluation Metric Details

The FairFace classifier outputs two gender categories, *male* and *female*, and seven race categories, *White*, *Southeast Asian*, *Middle Eastern*, *Latino*, *Hispanic*, *Indian*, *East Asian*, and *Black*. Based on these classification results, we compute the statistical parity against the target distributions. Table 10 shows the 2024 BLS employment statistics⁶ for *CEO*, *computer programmer*, *doctor*, *nurse*, and *housekeeper*. The original statistics report the percent of total employed for women, *White*, *Black or African American*, *Asian*, and *Hispanic or Latino*. To construct the BLS target distribution, we assigned the proportion of women to the probability of *female* and one minus that proportion to *male* in the gender category. For the race categories, we normalized the proportions for *White*, *Black or African American*, *Asian*, and *Hispanic or Latino* so that they sum to one⁷ and used this as the target distribution. Because the FairFace classifier does not include a generic *Asian* category, we combined the probabilities of *Southeast Asian* and *East Asian* to represent *Asian* when computing statistical parity.

⁶<https://www.bls.gov/cps/cpsaat11.htm>

⁷NOTE: Estimates for the above race groups (*White*, *Black or African American*, and *Asian*) do not sum to totals because data are not presented for all races. Persons whose ethnicity is identified as *Hispanic or Latino* may be of any race.

Table 12: Detected bias categories and corresponding attributes by different LLMs for the input prompt “A CEO”.

Category	Claude 3.7 Sonnet	GPT-4o	LLaMA 3.3	DeepSeek V3.2
Gender	male, female, non-binary	male, female, non-binary	male, female, non-binary	male, female, non-binary
Age	young, middle-aged, elderly	young adult, middle-aged, elderly	young adult, middle-aged, elderly	middle-aged, elderly, young adult
Race	White, Black, Asian, Hispanic, Middle Eastern, Indigenous	White, Asian, Black, Hispanic	White, Asian, Black, Hispanic, Middle Eastern	White, Asian, Black, Hispanic, Middle Eastern
Appearance / Attire	formal attire, business suit, casual business attire, professionally dressed	business suit, casual wear, formal wear	formal, business casual, luxurious, conservative, modern	well-dressed, formal attire, casual attire, professional
Body type / Physical ability	slim, athletic, average, plus-sized	–	–	able-bodied, uses mobility aid
Setting	office, boardroom, corporate headquarters, tech company, factory floor	boardroom, office, conference room	corporate, industrial, academic	–
Background	–	–	urban, rural	ivy league educated, self-made, inherited position, career climber
Pose	sitting at desk, standing, presenting, in meeting, speaking	–	–	–
Accessories	glasses, watch, briefcase, laptop, smartphone, tablet	–	–	–
Facial expression / Personality	serious, smiling, confident, authoritative, friendly	–	confident, serious, smiling, determined, approachable	authoritative, charismatic, decisive, collaborative
Industry / Environment	–	–	tech, finance, healthcare, manufacturing, services	technology, finance, healthcare, manufacturing, retail
Nationality	–	–	–	American, European, Asian, Global

C.2 ENTIGEN Setup Details

As an ethical intervention to promote equitable judgment in T2I models, we added “, *if all individuals can be β PROFESSION ζ irrespective of their gender and race*” to the end of the input prompt.

C.3 Fair Diffusion Setup Details

For gender editing, we predefined the prompts [“*male person*”, “*female person*”, “*non-binary person*”], and for race editing, the prompts [“*white person*”, “*black person*”, “*asian person*”, “*latino person*”, “*indian person*”]. During sampling, one gender prompt and one race prompt were drawn according to the target distribution, and `reverse_editing_direction=True` was used to enhance the selected attribute while suppressing the others. All editing operations employed the following hyperparameters (as in the original implementation):

Task Description
Please read the following task description carefully. If you do not follow the specified format, your answer will not be accepted.

Task
Read the descriptive text carefully. Think about what kinds of **biases** that could appear in an **image** (stereotypes, assumptions, or implicit characteristics) may be implied.

Important Rules

1. You must create **at least 2 categories**.
2. Each category must list **2 or more attributes**.
3. Try to list as many categories and attributes as you can think of.
4. Format must follow:
```\n category: attribute1, attribute2, ...\n category: attribute1, attribute2, ...\n ...```\n
5. **If you do not follow this format, your answer will be rejected.**

**Examples**

If the text is: "a firefighter"  
✓ **Correct format:**  
```\n gender: male, female, non-binary\n age: young adult, middle-aged, elderly\n race: White, Asian, Black, Hispanic\n ...```\n

✗ **Incorrect format:**
```\n race: Asian\n ...```\n

If the text is: "a quiet forest"  
✓ **Correct format:**  
```\n time\_of\_day: morning, afternoon, evening, night, dawn, dusk\n season: spring, summer, autumn, winter\n weather: sunny, cloudy, rainy, snowy, foggy, misty\n ...```\n

✗ **Incorrect format:**
```\n morning\n ...```\n

a graphic designer \*

Your answer

trees seen through a car window on a rainy day \*

Your answer

a head cook \*

Your answer

a grumpy porcupine handing a check for \$10 \*

Your answer

an industrial engineer \*

Your answer

a watermelon chair \*

Your answer

an interviewer \*

Your answer

Figure 7: The task interface shown to participants, including the task description, sample prompts, and entry fields for submitting responses.

- `edit_warmup_steps = 1`
- `edit_guidance_scale = 3.0`
- `edit_threshold = 0.95`
- `edit_weights = 1.0`
- `edit_momentum_scale = 0.3`
- `edit_momentum_beta = 0.6`

Except for these settings, all other parameters matched those of the original work Friedrich et al. [2023].

#### C.4 FairT2I Setup Details

T2I model sampling was performed using `PNDMScheduler` with 50 sampling steps. The `guidance_scale` for classifier-free guidance was set to 7.5. During inference, we set the batch size to 200 and image resolution  $512 \times 512$ , and a single inference on one NVIDIA H100 GPU took approximately 4 minutes.

For bias detection, we used `claude-3-7-sonnet-20250219`, and for prompt rewriting, we used `gpt-4o-mini-2024-07-18`.

The prompt used for LLM-assisted bias detection is as follows:

*Please read the following task description carefully. If you do not follow the specified format, your answer will not be accepted.*

**Task**

*Read the descriptive text carefully. Think about what kinds of biases that could appear in an image (stereotypes, assumptions, or implicit characteristics) may be implied.*

**Important Rules**

*You must create at least 2 categories.*

*Each category must list 2 or more attributes.*

*Try to list as many categories and attributes as you can think of.*

*Format must follow:*

```
{
 "category": ["attribute1", "attribute2", ...],
 "category": ["attribute1", "attribute2", ...],
}
```

*Do not include any text outside of the JSON output.*

*If you do not follow this format, your answer will be rejected.*

**Examples**

*If the text is: "a firefighter"*

*Correct format:*

```
{
 "gender": ["male", "female", "non-binary"],
 "age": ["young adult", "middle-aged", "elderly"],
 "race": ["White", "Asian", "Black", "Hispanic"],
}
```

*Incorrect format:*

```
{
 "race": "Asian"
}
```

*If the text is: "a quiet forest"*

*Correct format:*

```
{
 "time_of_day": ["morning", "afternoon", "evening", "night", "dawn", "dusk"],
 "season": ["spring", "summer", "autumn", "winter"],
 "weather": ["sunny", "cloudy", "rainy", "snowy", "foggy", "misty"],
}
```

*Incorrect format: morning*

The following prompt was used for the LLM-assisted fusion of the textual input **y** and the latent attribute **z**:

*Please read the following task description carefully. If you do not follow the specified format, your answer will not be accepted.*

**Task**

*Rewrite the original prompt so that it naturally integrates all specified attributes.*

**Important Rules**

- *Output must contain only the rewritten prompt text.*
- *Do not add, expand, or explain beyond the original prompt and attributes.*
- *Do not include extra descriptive words, embellishments, or commentary.*
- *Do not include explanations, metadata, or formatting outside of the rewritten prompt.*
- *The rewritten sentence must be as concise as possible, while preserving the original meaning and smoothly integrating all attributes.*

**Format**

*<rewritten prompt text>*

*If you do not follow this format, your answer will be rejected.*

**Examples**

*If the input is:*

{  
*Original prompt: "A portrait of a person reading a book"*  
*Attributes to include: "gender: female, age: elderly"*  
 }

*Correct format:*

{  
*A portrait of an elderly female person reading a book*  
 }

*Incorrect format:*

{  
*A detailed portrait depicting an elderly female person seated in a quiet and serene setting, holding a book gently in her hands while reading it with focused attention and calm concentration.*  
 }

## C.5 Statistical Significance Test Methodology

To determine if FairT2I achieved statistically significantly lower SP scores compared to another method (denoted as Method A), we employed a one-sided non-parametric bootstrap hypothesis test with  $N_{boot} = 1000$  iterations. In each iteration  $i$ , demographic classifications were resampled with replacement from the set of generated images for Method A and FairT2I, maintaining the original sample sizes from which the SP scores were computed. Specifically:

- For the **uniform distribution target** (see subsection C.6), overall SP scores were initially calculated from demographic classifications of all 50 occupations  $\times$  200 images/occupation = 10,000 images generated per method. The bootstrap procedure then resampled from these 10,000 image classifications for each method to generate bootstrap SP scores.
- For the **BLS statistics target** (see subsection C.8), SP scores were initially calculated for each occupation based on the  $n = 200$  images generated per occupation per method. The bootstrap procedure then resampled from the 200 image classifications for a given occupation for each method.

SP scores were then calculated for these bootstrap samples ( $SP_{A,i}^*$  for Method A and  $SP_{B,i}^*$  for FairT2I, where B denotes FairT2I). The difference  $D_i^* = SP_{A,i}^* - SP_{B,i}^*$  was computed for each iteration. The  $p$ -value was estimated as the proportion of these bootstrap differences  $D_i^*$  that were less than or equal to zero:  $p = \frac{\sum_{i=1}^{N_{boot}} \mathbb{I}(D_i^* \leq 0)}{N_{boot}}$ , where  $\mathbb{I}(\cdot)$  is the indicator function. This



Figure 8: Generated images for the input text “*a headshot of a psychologist*” by the original Stable Diffusion, ENTIGEN, FairDiffusion, and FairT2I (Ours).

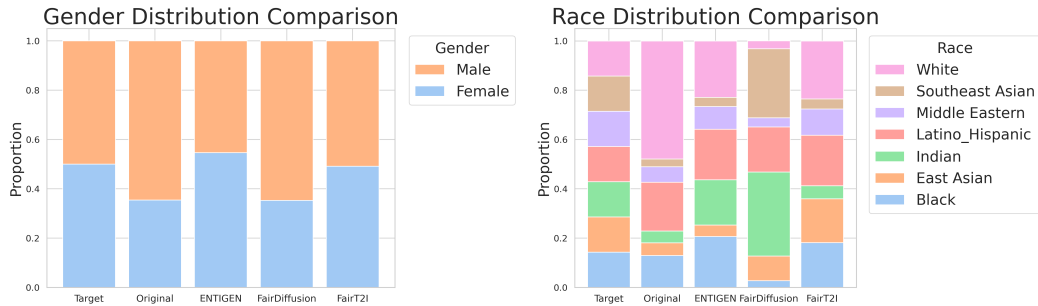


Figure 9: Comparison of the target uniform distribution and empirical distributions produced by original Stable Diffusion, ENTIGEN, FairDiffusion and FairT2I (Ours) for gender (left) and race (right), shown as stacked bar charts.

*p*-value tests the null hypothesis  $H_0 : \text{SP}_{\text{FairT2I}} \geq \text{SP}_{\text{Method A}}$  against the alternative hypothesis  $H_A : \text{SP}_{\text{FairT2I}} < \text{SP}_{\text{Method A}}$ .  $p < 0.05$  indicates that FairT2I is significantly better than Method A for the given SP metric.

### C.6 Detailed Results of Uniform Distribution Target

The overall SP scores for gender and race when targeting a uniform distribution are presented in Table 13. The statistical significance of FairT2I’s scores compared to other methods was assessed using the bootstrap test described in subsection C.5.

Table 13: Gender SP (left) and Race SP (right) scores (lower is better) from the uniform distribution. For each metric, the best score is shown in **bold**. For Original, ENTIGEN, and FairDiffusion, the *p*-value in parentheses (*p*-val) indicates if FairT2I (Ours) is significantly better than that method ( $p < 0.05$  highlighted in **bold** for  $\text{SP}_{\text{FairT2I}} < \text{SP}_{\text{Method}}$ ).

Method	Gender SP ↓	Race SP ↓
Original	0.2056 ( <b>&lt;0.0001</b> )	0.3907 ( <b>&lt;0.0001</b> )
ENTIGEN	0.0661 ( <b>&lt;0.0001</b> )	0.2001 ( <b>&lt;0.0001</b> )
FairDiffusion	0.2083 ( <b>&lt;0.0001</b> )	0.3137 ( <b>&lt;0.0001</b> )
FairT2I (Ours)	<b>0.0123</b>	<b>0.1864</b>

### C.7 Evaluation Results

**Discussion of uniform distribution results** As shown in Table 13, when targeting a uniform demographic distribution across all occupations, FairT2I (Ours) achieved the best overall SP scores for both Gender SP (0.0123) and Race SP (0.1864). The statistical significance tests, detailed in subsection C.5, confirm these improvements. FairT2I is shown to be significantly better than the Original method (Gender SP: 0.2056, Race SP: 0.3907), ENTIGEN (Gender SP: 0.0661, Race SP:

Table 14: Gender SP (top) and Race SP (bottom) scores (lower is better) when targeting BLS statistics. For each metric and occupation, the best score is shown in **bold**. For Original, ENTIGEN, and FairDiffusion, the  $p$ -value in parentheses ( $p$ -val) indicates if FairT2I (Ours) is significantly better than that method ( $p < 0.05$  highlighted in **bold** for  $SP_{\text{FairT2I}} < SP_{\text{Method}}$ ).

<b>Method</b>	Gender SP ↓				
	CEO	comp. prog.	doctor	nurse	housekeeper
Original	0.3637 <b>(0.000)</b>	0.1651 <b>(0.000)</b>	0.3843 <b>(0.000)</b>	0.1796 <b>(0.001)</b>	0.1459 <b>(0.000)</b>
ENTIGEN	0.3748 <b>(0.000)</b>	0.0569 (0.254)	0.1229 (0.123)	0.1210 <b>(0.044)</b>	<b>0.0121</b> (0.547)
FairDiffusion	0.1956 <b>(0.022)</b>	0.1089 <b>(0.044)</b>	0.1138 (0.206)	0.1653 <b>(0.004)</b>	0.1597 <b>(0.000)</b>
FairT2I (Ours)	<b>0.0710</b>	<b>0.0170</b>	<b>0.0550</b>	<b>0.0537</b>	<b>0.0121</b>
<b>Method</b>	Race SP ↓				
	CEO	comp. prog.	doctor	nurse	housekeeper
Original	0.6050 <b>(0.000)</b>	0.2213 <b>(0.003)</b>	0.2110 <b>(0.016)</b>	0.1971 (0.234)	1.0207 <b>(0.000)</b>
ENTIGEN	0.5004 <b>(0.000)</b>	0.6115 <b>(0.000)</b>	0.4727 <b>(0.000)</b>	0.4805 <b>(0.000)</b>	0.9341 <b>(0.000)</b>
FairDiffusion	0.1664 <b>(0.019)</b>	0.1484 <b>(0.027)</b>	<b>0.0750</b> (0.752)	<b>0.1285</b> (0.714)	0.3074 <b>(0.008)</b>
FairT2I (Ours)	<b>0.0677</b>	<b>0.0886</b>	0.1137	0.1540	<b>0.2001</b>

0.2001), and FairDiffusion (Gender SP: 0.2083, Race SP: 0.3137) for both metrics, with all associated  $p$ -values being less than 0.000. This indicates a strong and statistically robust improvement in fairness for overall image generation when a uniform distribution is the goal.

**Stacked Bar-Chart Visualization** Figure 9 presents a stacked bar-chart comparison between the target uniform distribution and the empirical distributions produced by Stable Diffusion, ENTIGEN, Fair Diffusion, and our proposed FairT2I. Among these methods, FairT2I demonstrates the closest alignment with the target distribution.

### C.8 Detailed Results of BLS Statistics Target

For the BLS statistics target, FairT2I’s performance in achieving lower SP scores per occupation was also evaluated against other methods. The statistical significance of these comparisons was determined using the one-sided non-parametric bootstrap hypothesis test detailed in subsection C.5. The SP scores and the corresponding  $p$ -values from these tests are presented in Table 14.

**Discussion of BLS statistics results** The analyses in Table 14 indicate that FairT2I generally achieves lower SP scores for both gender and race attributes compared to existing methods when targeting BLS statistics. For **Gender SP**, FairT2I consistently demonstrates statistically significant improvements ( $p < 0.05$ ) over the Original method across all five occupations. It also shows significant advantages over FairDiffusion in most occupations (*CEO, computer programmer, nurse, housekeeper*). Compared to ENTIGEN, FairT2I provides significant improvements in two occupations (*CEO, nurse*), while for others, including a tied best performance with ENTIGEN for *housekeeper*, the differences were not statistically significant. Regarding **Race SP**, FairT2I shows robust and statistically significant improvements over ENTIGEN across all occupations. Against the Original method, FairT2I is significantly better in four out of five occupations. When compared with FairDiffusion, FairT2I offers significant gains for three occupations (*CEO, computer programmer, housekeeper*). Notably, FairDiffusion achieved lower Race SP scores for the *doctor* and *nurse* occupations, where FairT2I did not show a significant advantage.

**Stacked bar chart visualization** Figure 10 presents stacked bar charts comparing demographic distributions of target BLS statistics and empirical distributions across five occupations. Visually, FairT2I generally demonstrates a closer alignment to the target BLS distributions for both gender and race across most occupations.

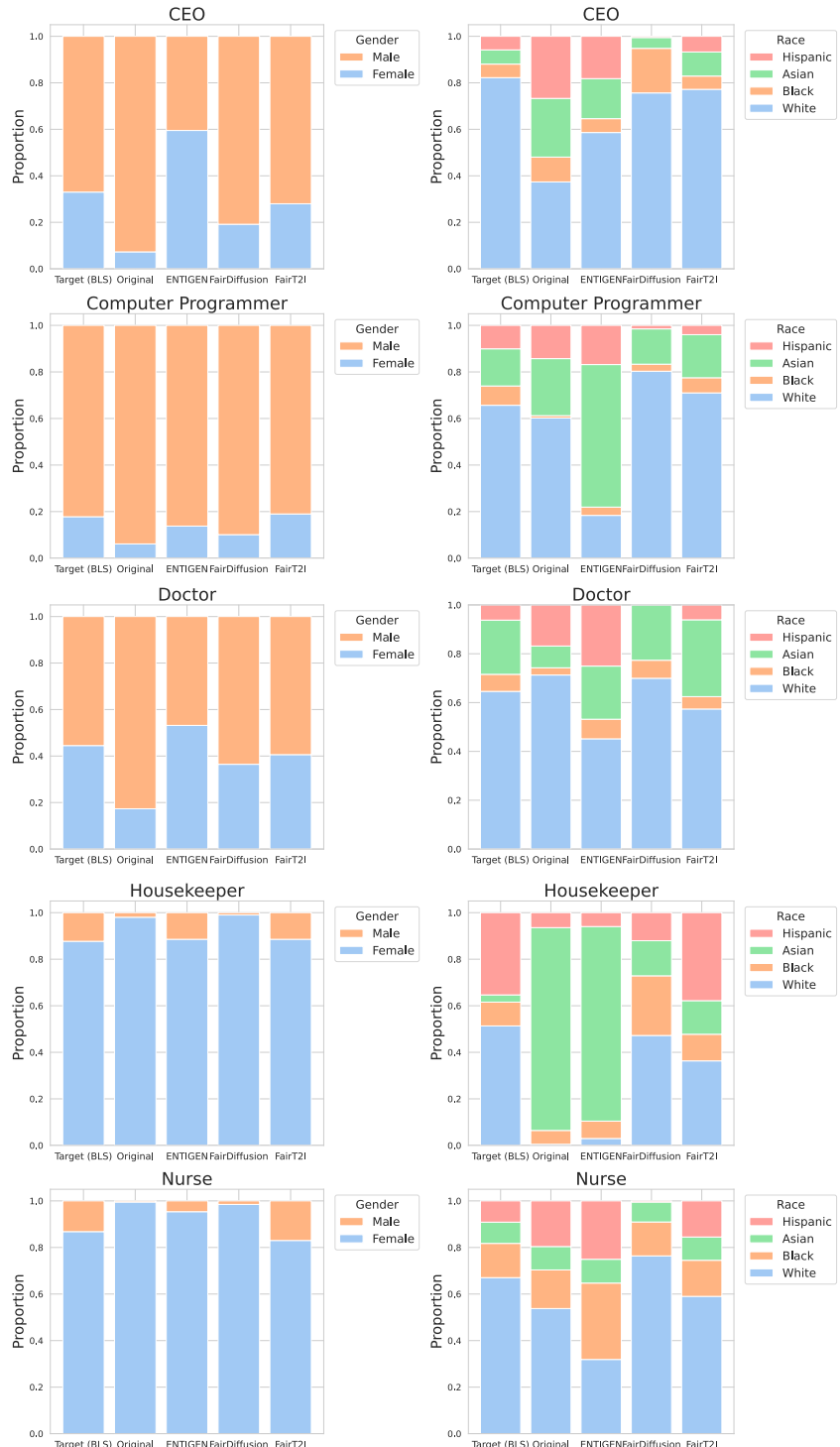


Figure 10: Comparison of the target BLS statistics and empirical distributions produced by original Stable Diffusion, ENTIGEN, FairDiffusion and FairT2I (Ours) for gender (left) and race (right), shown as stacked bar charts.

## D Details for Diversity Control Experiment

### D.1 Evaluation Metrics Details

This section provides further details on the implementation of the evaluation metrics used in Section 6 to assess image fidelity, text-image alignment, and diversity. For all trace-based diversity metrics, we generated 200 images for each of the 50 sampled Parti Prompts. Image features were extracted from these 200 images, and the trace of their covariance matrix was computed.

**FID.** We calculated FID Heusel et al. [2017] to assess image fidelity against the COCO Karpathy test split [Lin et al., 2014]. We used the PyTorch implementation of FID from the `pytorch-fid` library<sup>8</sup>.

**CLIPScore.** To evaluate text-image alignment, we computed CLIPScore Hessel et al. [2021].

- **Model and Library:** We utilized the OpenAI CLIP ViT-B/32 model, accessed via the official `clip` Python package.
- **Feature Extraction:** For each (prompt, generated image) pair, the prompt text was encoded using `model.encode_text()` and the image was encoded using `model.encode_image()`. Both encoders produce L2-normalized features.
- **Score Calculation:** The CLIPScore for a single pair is the dot product of their respective normalized feature embeddings.
- **Aggregation:** The final reported CLIPScore for a given prompt is the average score across all 200 images generated for that prompt.

**CLIP Trace.** To quantify diversity using CLIP Radford et al. [2021] features, we calculated the trace of the covariance matrix of image embeddings.

- **Model and Library:** We used the OpenAI CLIP ViT-B/32 model, via the `clip` Python package.
- **Feature Extraction:** For each of the 50 sampled prompts, we generated 200 images. All 200 images were encoded into L2-normalized feature vectors using `model.encode_image()` with a batch size of 32. This resulted in a set of 200 feature vectors per prompt.
- **Trace Calculation:** For each prompt, we computed the covariance matrix of these 200 feature vectors using `numpy.cov(features, rowvar=False)`. The CLIP Trace diversity metric is the trace of this covariance matrix, calculated using `numpy.trace()`.

**BLIP2 Trace.** Similar to CLIP Trace, we also quantified diversity using BLIP-2 Li et al. [2023] features.

- **Model and Library:** We employed the `Salesforce/blip2-opt-2.7b` model, accessed via the Hugging Face `transformers` library, specifically using `Blip2Processor` for preprocessing and `Blip2Model` for feature extraction.
- **Feature Extraction:** For each prompt, the 200 generated images were processed. Image features were obtained from the `pooler_output` of `model.get_image_features()`.
- **Trace Calculation:** Analogous to CLIP Trace, for each prompt, we computed the covariance matrix of the 200 BLIP-2 image feature vectors and then calculated its trace.

### D.2 FairT2I Setup Details

T2I model sampling was performed using `FlowMatchEulerDiscreteScheduler` with 28 sampling steps. The `guidance_scale` for classifier-free guidance was set to 4.0. During inference, we set the batch size to 200 and image resolution  $1024 \times 1024$ , and a single inference on one NVIDIA H100 GPU took approximately 4 minutes. For bias detection, we used `claude-3-7-sonnet-20250219`, and for prompt rewriting, we used `gpt-4o-mini-2024-07-18`.

<sup>8</sup><https://github.com/mseitzer/pytorch-fid>

The same prompt in subsection C.4 was used for LLM-assisted bias detection is as follows. We utilized the same prompt for integration of the input text  $y$  and the sensitive attribute  $z$  with subsection C.4.

### D.3 Statistical Significance Test Methodology

To assess the statistical significance of the differences observed in diversity (BLIP2 Trace, CLIP Trace) and text-image alignment (CLIP Score) metrics (see section 6 in the main paper), we performed one-sided Mann-Whitney U tests. This non-parametric test was chosen as it does not assume a specific distribution (e.g., normality) for the data and is suitable for comparing two independent samples of per-prompt scores. For each comparison between two methods (Group 1 and Group 2, as detailed in Table 15), we tested the alternative hypothesis ( $H_A$ ) that the scores from Group 1 are stochastically greater than those from Group 2. The detailed results of these tests, including  $p$ -values and findings, are presented in Table 15. Note that statistical tests for FID scores were not performed due to the high computational cost associated with generating multiple full sets of images for each condition required for robust FID variance estimation. FID scores are reported as single values based on one comprehensive generation run per method.

### D.4 Discussion of Diversity, Alignment, and Fidelity Results

The statistical analyses presented in Table 15, along with reported FID scores, provide insights into FairT2I’s performance in terms of image diversity, text-image alignment, and image fidelity, relative to baseline Stable Diffusion models with varying classifier-free guidance (CFG) scales.

**Diversity (Trace Scores)** FairT2I (itself using a CFG scale of 4.0) demonstrates a statistically significant increase in diversity, as measured by both BLIP2 Trace and CLIP Trace, when compared to the original Stable Diffusion model using higher or equivalent CFG scales (i.e., CFG 7.0 and CFG 4.0). Specifically, for both trace metrics, FairT2I’s scores were significantly higher (all  $p < 0.00001$ , except for BLIP2 Trace vs. Original CFG 4.0 where  $p = 0.000002$ ). When compared to the original model with a very low CFG scale (CFG 1.0), which typically yields high diversity, the results are nuanced. While the original CFG 1.0 model achieved numerically higher mean trace scores for both BLIP2 Trace and CLIP Trace compared to FairT2I, these differences were not found to be statistically significant (BLIP2 Trace  $p = 0.255$ ; CLIP Trace  $p = 0.069$  when testing  $H_A$ : Original CFG 1.0 > FairT2I). This suggests FairT2I achieves a level of diversity that is statistically comparable to that of the highly diverse CFG 1.0 setting.

**Text-image alignment (CLIP Score)** For CLIP Scores, the original model with CFG scales of 7.0 and 4.0 yielded statistically significantly higher scores than FairT2I ( $p = 0.021$  and  $p = 0.008$ , respectively, when testing  $H_A$ : Original > FairT2I). This indicates a slight, yet statistically significant, decrease in text-image alignment for FairT2I when compared to these higher CFG scale baselines. However, when comparing FairT2I to the original model with CFG 1.0, there was no statistically significant evidence that Original CFG 1.0’s CLIP Score was higher than FairT2I’s ( $p = 0.664$ ). Numerically, FairT2I’s mean CLIP Score was slightly higher than that of Original CFG 1.0. This suggests a trade-off: increasing diversity via FairT2I might involve a small compromise in text-image alignment relative to high-guidance settings, but the alignment remains competitive, especially when compared to other high-diversity configurations like CFG 1.0.

**Image Fidelity (FID) and overall balance** While statistical tests were not performed for FID due to computational expense, the reported scores (Original CFG 7.0: 27.13, Original CFG 4.0: 26.46, Original CFG 1.0: 34.47, FairT2I: 26.24) indicate that FairT2I achieves the best image fidelity (lowest FID score). It surpasses or matches the fidelity of the original model at CFG 4.0 and 7.0, and is substantially better than the CFG 1.0 setting, which shows a marked degradation in fidelity.

**Conclusion on trade-offs** Taken together, FairT2I appears to offer a favorable balance. It significantly enhances image diversity over standard CFG settings (4.0 and 7.0) and achieves diversity levels statistically comparable to the very low CFG 1.0 setting. While there is a statistically significant, albeit modest, reduction in CLIPScore compared to using CFG 4.0 and 7.0 with the original model, FairT2I maintains excellent image fidelity (best FID). This presents a notable advantage over simply lowering the CFG scale to 1.0 with the original model, which boosts diversity but at

a considerable cost to image fidelity and without a clear advantage in text-image alignment over FairT2I. Therefore, FairT2I effectively increases diversity while largely preserving image quality and maintaining a competitive level of text-image alignment.

Table 15: Statistical comparison of FairT2I with Original Stable Diffusion (various CFG scales) using one-sided Mann-Whitney U tests. For all comparisons, the alternative hypothesis ( $H_A$ ) tested is that the median score of **Group 1** is stochastically greater than that of **Group 2**. Significance level  $\alpha = 0.05$ .

Metric	Group 1	Group 2	p-value	Finding
BLIP2 Trace	FairT2I	CFG 7.0	<0.000001	Group 1 significantly higher
	FairT2I	CFG 4.0	0.000002	Group 1 significantly higher
	CFG 1.0	CFG 4.0	0.255153	Group 1 not significantly higher
CLIP Trace	FairT2I	CFG 7.0	<0.000001	Group 1 significantly higher
	FairT2I	CFG 4.0	<0.000001	Group 1 significantly higher
	CFG 1.0	CFG 4.0	0.068690	Group 1 not significantly higher
CLIP Score	CFG 7.0	FairT2I	0.020644	Group 1 significantly higher
	CFG 4.0	FairT2I	0.008392	Group 1 significantly higher
	CFG 1.0	FairT2I	0.664210	Group 1 not significantly higher

## D.5 User Study Details

We conducted a user study using the crowdsourcing platform *Prolific* to collect annotations from a diverse group of participants. Prolific allows researchers to recruit participants according to pre-defined demographic quotas; in our case, we applied *sex* and *ethnicity* quotas to ensure balanced participation and obtain responses from a demographically varied pool of annotators.

All responses were collected via a *Google Form*. For each task, participants were presented with a text prompt and sets of images generated by four anonymized models (*Model A*, *Model B*, *Model C*, and *Model D*). They were asked to rate each model on a five-point Likert scale (1 = worst, 5 = best) along three criteria: *diversity*, *image quality*, and *text–image alignment*. Each model output was displayed as a  $3 \times 3$  image grid aligned horizontally with white padding to facilitate visual comparison.

To promote consistent and reliable responses, the instruction section included concise explanations and rubrics defining each evaluation criterion. The complete task interface shown to participants is illustrated in Figure 11. Additionally, we enforced a regular-expression-based input format to ensure well-structured and standardized annotations across all responses.

We sampled 50 prompts from the Parti Prompts dataset [Yu et al., 2022], as detailed in subsection B.1. To keep the annotation workload manageable, these 50 prompts were divided into five separate tasks, each containing 10 prompts. Each task was assigned to a distinct group of participants to prevent repetition across annotators.

For each task, we recruited 20 independent annotators, resulting in a total of 100 participants overall. This configuration maintained an average completion time of approximately 20 minutes per participant. Each participant received an hourly rate of approximately **£6.0**, which is slightly below Prolific’s recommended fair payment rate but was deemed reasonable given the short task duration and minimal cognitive load.

## D.6 Visual Results

This section presents additional visual comparisons for several input text prompts in Parti Prompt dataset. Figures 12–15 illustrate images generated using our proposed FairT2I method alongside those generated with classifier-free guidance (CFG) at varying scales (7.0, 4.0, and 1.0). As noted in the captions, a guidance scale of 1.0 effectively corresponds to generation without the influence of classifier-free guidance. Our FairT2I method demonstrates an enhanced capability to diversify generation results, particularly for prompts that do not necessarily involve humans—spanning categories such as animals (Figures 12 and 15), objects (Figure 13), and abstract concepts (Figure

**Task Description**  
Please read the following task description carefully. If you do not follow the specified format, your answer will not be accepted.

**Task**

In this survey, you will be asked to **evaluate images generated by different models** (labeled as **Model A–D**).

For each prompt, you will see a grid of **9 images per model**, displayed side by side (horizontally concatenated across the four models). Please **rate each model independently** according to the given criterion (**Diversity**, **Image Quality**, or **Text Alignment**) on a **1–5 scale**.

Your ratings should reflect how well each model performs on the specific criterion, using the full range of the scale where appropriate.

**Important Rules**

1. Please evaluate **each model independently** on the provided 1–5 scale.
2. Use the **entire scale**: 1 = very poor, 5 = excellent, with intermediate values (2–4) for partial cases.
3. Do **not** assign the same score automatically to all models; instead, consider the **specific differences** in diversity, quality, or alignment for each model.
4. Responses that show too careless or too uniform scoring (e.g., always selecting the same number for all models) may not be accepted.

**Evaluation criteria:**

- **Diversity**: How different the multiple images from the same model look for the same prompt. High diversity means the images show clearly different variations (e.g., viewpoint, layout, details), while low diversity means the images look nearly identical.
- **Image Quality**: How clear, coherent, and visually convincing the image looks within its intended style. High quality images are sharp, well-structured, and free from obvious AI artifacts (e.g., severe distortions, broken anatomy, unnatural textures), even if the content is fantastical or stylized (e.g., anime, surreal objects).
- **Alignment**: How well the generated image matches the prompt in terms of objects, attributes, and relationships.

a pile of cash on a wooden table



Model A      Model B      Model C      Model D

Diversity \*

1 = Almost identical outputs: Images look the same with no meaningful variation.  
2 = Limited diversity: Only minor differences (e.g., small color or texture changes), overall very similar.  
3 = Moderate diversity: Some noticeable differences, but repetition is still common.  
4 = Good diversity: Several clearly distinct variations with minor overlap.  
5 = Strong diversity: Images show strong and consistent variety in viewpoint, layout, or details, with minimal repetition.

	1. Almost identical outputs	2. Limited diversity	3. Moderate diversity	4. Good diversity	5. Strong diversity
Model A	<input type="radio"/>	<input type="radio"/>	<input type="radio"/>	<input type="radio"/>	<input type="radio"/>
Model B	<input type="radio"/>	<input type="radio"/>	<input type="radio"/>	<input type="radio"/>	<input type="radio"/>
Model C	<input type="radio"/>	<input type="radio"/>	<input type="radio"/>	<input type="radio"/>	<input type="radio"/>
Model D	<input type="radio"/>	<input type="radio"/>	<input type="radio"/>	<input type="radio"/>	<input type="radio"/>

Figure 11: User study interface provided to participants, including the task description, input prompts, generated images, and the multi-grid answer form for annotators.

14). Each figure allows for a qualitative assessment of the different generation conditions for its respective prompt.

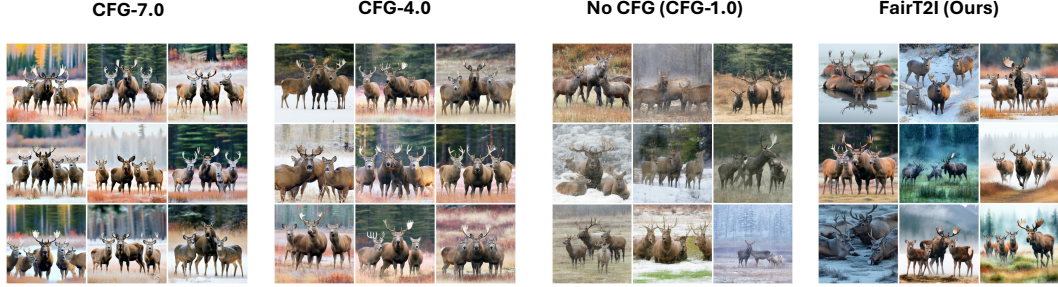


Figure 12: Generated images for the input text “*Four deer surrounding a moose.*” by classifier-free guidance (CFG) at guidance scales 7.0, 4.0, and 1.0 and FairT2I (Ours). A guidance scale of 1.0 corresponds to generation without CFG.



Figure 13: Generated images for the input text “*a Ferrari Testarossa in front of the Kremlin*” by classifier-free guidance (CFG) at guidance scales 7.0, 4.0, and 1.0 and FairT2I (Ours). A guidance scale of 1.0 corresponds to generation without CFG.



Figure 14: Generated images for the input text “*meaning of life*” by classifier-free guidance (CFG) at guidance scales 7.0, 4.0, and 1.0 and FairT2I (Ours). A guidance scale of 1.0 corresponds to generation without CFG.

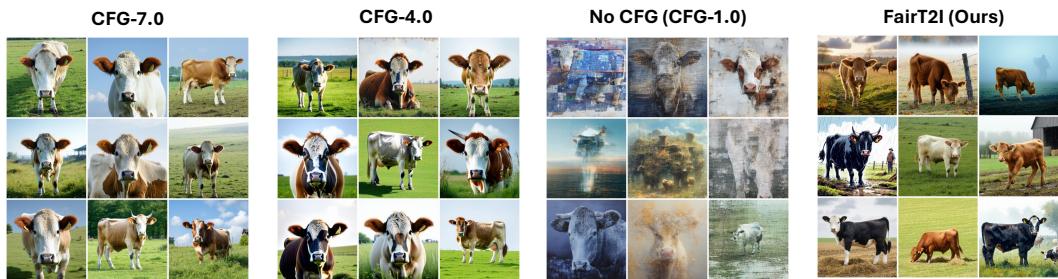


Figure 15: Generated images for the input text “*a cow*” by classifier-free guidance (CFG) at guidance scales 7.0, 4.0, and 1.0 and FairT2I (Ours). A guidance scale of 1.0 corresponds to generation without CFG.